

# Generative Models in Computational Pathology: A Comprehensive Survey on Methods, Applications, and Challenges

Yuan Zhang, Xinfeng Zhang, Xiaoming Qi, Xinyu Wu, Feng Chen, Guanyu Yang, *Senior Member, IEEE*, and Huazhu Fu, *Senior Member, IEEE*

arXiv:2505.10993v1 [eess.IV] 16 May 2025

**Abstract**—Generative modeling has emerged as a promising direction in computational pathology, offering capabilities such as data-efficient learning, synthetic data augmentation, and multi-modal representation across diverse diagnostic tasks. This review provides a comprehensive synthesis of recent progress in the field, organized into four key domains: image generation, text generation, multimodal image–text generation, and other generative applications, including spatial simulation and molecular inference. By analyzing over 150 representative studies, we trace the evolution of generative architectures—from early generative adversarial networks to recent advances in diffusion models and foundation models with generative capabilities. We further examine the datasets and evaluation protocols commonly used in this domain and highlight ongoing limitations, including challenges in generating high-fidelity whole slide images, clinical interpretability, and concerns related to the ethical and legal implications of synthetic data. The review concludes with a discussion of open challenges and prospective research directions, with an emphasis on developing unified, multimodal, and clinically deployable generative systems. This work aims to provide a foundational reference for researchers and practitioners developing and applying generative models in computational pathology.

**Index Terms**—Computational Pathology, Generative Model, Diffusion Model, Generative Adversarial Network

## I. INTRODUCTION

Generative models have become a transformative force in medical image analysis, offering capabilities that extend beyond traditional discriminative learning [1], [2]. By modeling complex data distributions, these models can synthesize high-fidelity images and enable a wide range of downstream tasks, such as data augmentation, cross-modal translation, and representation learning [3]. Their utility is especially pronounced in computational pathology, a domain characterized by high-resolution whole-slide images (WSIs), heterogeneous tissue morphology, and significant annotation burdens.

Computational pathology has rapidly evolved into a data-intensive field driven by advances in deep learning and whole slide imaging [4]. However, this progress also reveals core limitations in data availability, generalization, and robustness across clinical domains [5]. Generative models such as generative adversarial networks (GAN),

Yuan Zhang and Xinfeng Zhang contributed equally to this work. Corresponding author: Guanyu Yang and Huazhu Fu.

Y. Zhang and G. Yang are with the Key Laboratory of New Generation Artificial Intelligence Technology and Its Interdisciplinary Applications (Southeast University), Ministry of Education, Nanjing, China (e-mail: yuanzhang@seu.edu.cn, yang.list@seu.edu.cn).

X. Zhang is with the School of Biomedical Engineering, Tsinghua University, Beijing, China (e-mail: zhang-xf22@mails.tsinghua.edu.cn).

X. Qi is with the Department of Biomedical Engineering and Department of Electrical and Computer Engineering, National University of Singapore, Singapore, Singapore (e-mail: qixiaoming12138@163.com).

X. Wu is with the School of Information Science and Engineering, Southeast University, Nanjing, China (e-mail: xinyuwu@seu.edu.cn).

F. Chen is with the Department of Biostatistics, Center for Global Health, School of Public Health, Nanjing Medical University, Nanjing, China (e-mail: fengchen@njmu.edu.cn).

H. Fu is with Institute of High-Performance Computing, Agency for Science, Technology and Research, Singapore (e-mail: hzfu@iee.org).

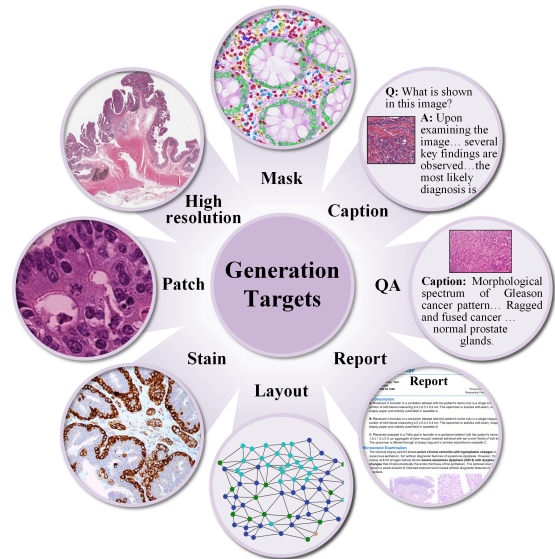


Fig. 1. Illustration of diverse generative targets in computational pathology, covering a wide spectrum ranging from image synthesis and mask generation to textual reports and spatial or question answering.

variational autoencoders (VAE), diffusion models, and foundation models like large language models (LLM) and vision-language models (VLM) have proven effective in addressing these challenges. These models support a wide range of applications, including synthetic data generation, stain normalization, style transfer, tissue synthesis, and rare pathology simulation, thereby enhancing learning-based approaches under data-scarce or domain-shifted conditions.

Research on generative models in pathology has grown rapidly, as illustrated in Fig. 3. After a period of sparse, exploratory studies, publication volume increased steadily, with a sharp rise from 2024 onward. This inflection point marks a broader shift in the field, as researchers increasingly recognize the unique advantages that generative models offer in addressing long-standing challenges in digital pathology, including limited data availability, high annotation costs, and the demand for high-fidelity, consistent synthetic images.

Despite the rapid proliferation of generative approaches in pathology, a focused and comprehensive review that systematizes existing methods and contextualizes their impact remains absent. Prior reviews in computer vision often address generative models from a broad or algorithm-centric perspective [6], [7], leaving the unique challenges and opportunities in pathology underexplored. Given the domain-specific demands of pathology, such as cell-level structural fidelity, high-resolution WSI, and stain consistency, there is a pressing need to consolidate current developments under a pathology-centric lens. Furthermore, with the advent of foundation models and cross-modal generation strategies, the generative paradigm in pathology is undergoing a significant shift, warranting timely reflection and synthesis.

In this survey, we present a comprehensive and systematic overview of generative models in computational pathology. We ana-

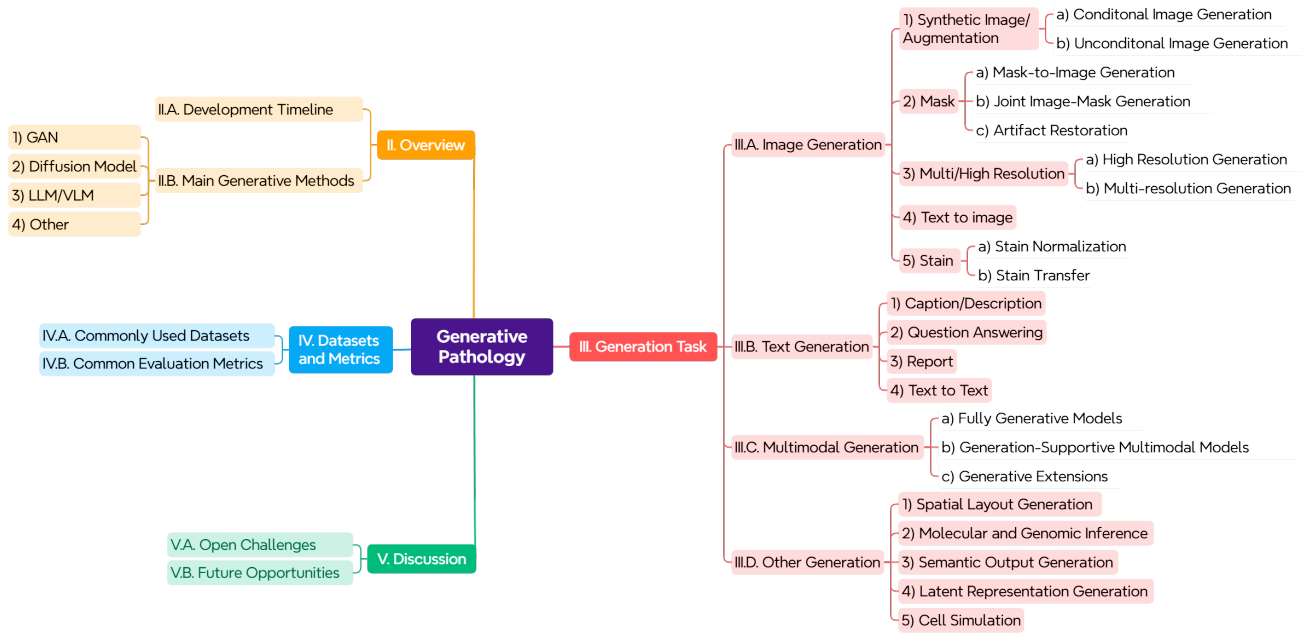


Fig. 2. Conceptual map of generative modeling tasks in computational pathology. This figure outlines the overall structure of the survey, categorizing generative methods into four major domains: image generation, text generation, multimodal generation, and other emerging modalities. Subtasks such as stain normalization, high resolution image synthesis, report generation, and spatial layout generation are grouped to reflect the breadth and evolution of generative capabilities in the field.

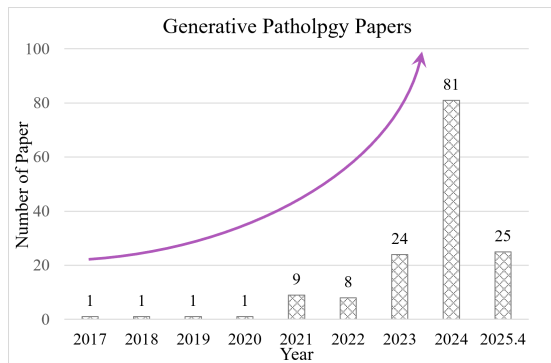


Fig. 3. Number of published papers related to generative models in pathology over time. The purple curve represents an exponential trend line, highlighting the accelerating growth of research interest in this field.

lyze over 150 peer-reviewed papers, encompassing diverse generative targets, as shown in Fig. 1. To facilitate a structured understanding of this rapidly evolving field, we propose a multi-dimensional taxonomy that categorizes existing works according to generation targets, algorithmic approaches, application tasks, and relevant datasets. Our review adopts a hierarchical framework that begins with generation targets before systematically examining specific tasks and their corresponding methodologies in Fig. 2. Specifically, we detail the methodological evolution of generative models across major pathology tasks such as synthetic image, text, and multimodal generation. Within image generation, we distinguish between downstream tasks such as synthetic image creation, image-mask pair generation, high-resolution synthesis, stain transfer, and cross-modality translation. For text generation, we cover captioning, report generation, and question answering. Multimodal generation involves the use of foundation models to enable cross-modal transformation and generation across

images, text, and other clinical data modalities. We then survey representative generative models, such as GANs, VAEs, and diffusion models, along with their design objectives and performance trade-offs. Furthermore, we consolidate information on commonly used datasets and evaluation metrics, thereby providing an essential resource for researchers entering this field. Finally, we identify current limitations and outline promising future directions, including clinically grounded generation, interpretable generation, and integration with foundation models. This hierarchical organization allows us to not only highlight the diversity of generative objectives in pathology but also to reveal methodological trends across different data modalities and clinical applications. We hope this work provides a roadmap for the researchers to explore the field further.

Our major contributions include:

- To our knowledge, this is the first comprehensive survey that systematically reviews generative models in computational pathology, covering over 150 publications up to April 2025 across diverse generative paradigms.
- We propose a unified taxonomy that organizes generative pathology research by generation targets and modeling approaches, offering a structured perspective on how generative methods address key challenges in pathology synthesis.
- We compile a curated summary of commonly used datasets and evaluation protocols across different pathology generation tasks.
- We critically discuss the open challenges in generative pathology and highlight future directions.

The remainder of this survey is organized as follows. Section II provides an overview of representative generative models applied to computational pathology, along with a historical timeline of their development. Section III categorizes the key applications of generative methods in computational pathology, including image generation, text generation, multimodal generation, and other emerging tasks. Section IV reviews widely used datasets for training generative

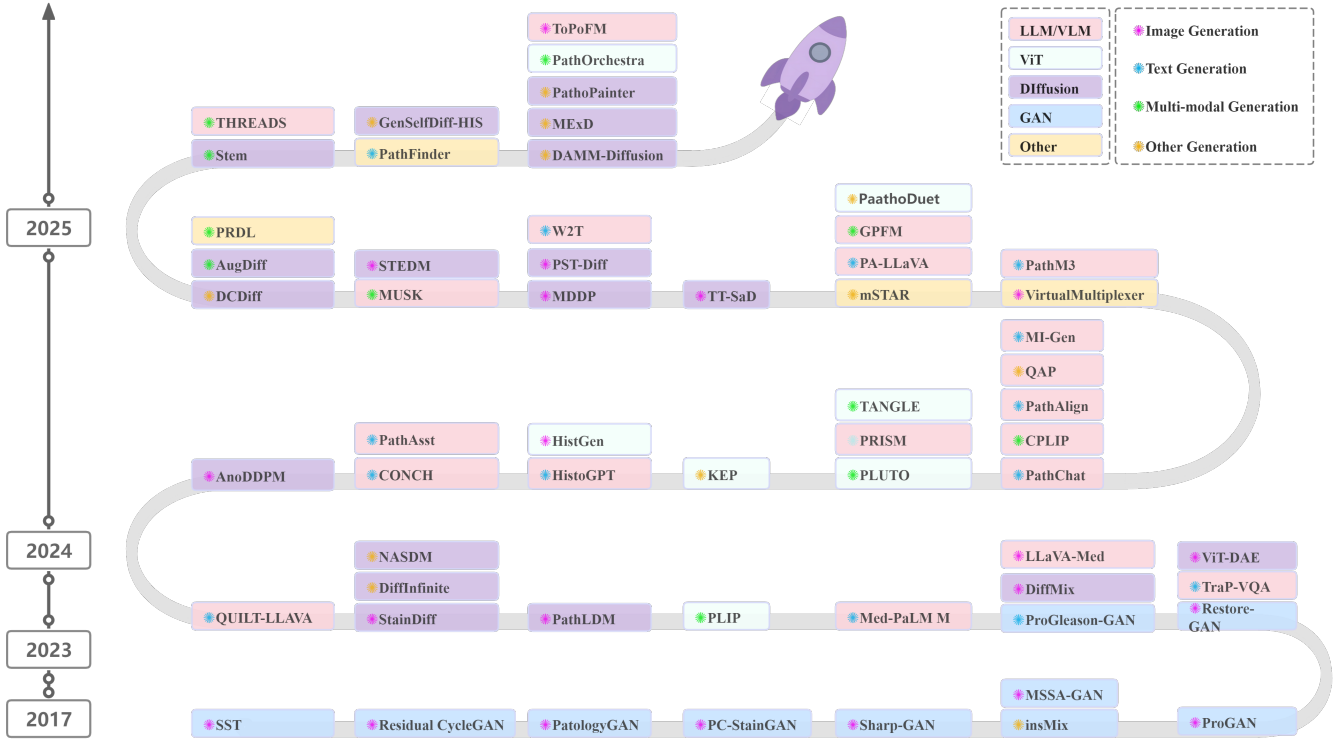


Fig. 4. Timeline of representative generative methods in computational pathology (2017-2025), reflecting the growing interest and diversification of generative modeling techniques for image, text, multimodal, and other applications within the field.

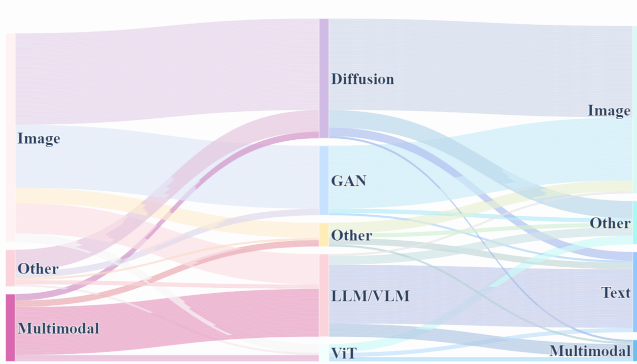


Fig. 5. The flow of information from input modalities, through diverse model architectures, to output modalities represents the current distribution of generative models in computational pathology.

models and common evaluation metrics. Finally, Section V discusses the broader impact of generative models in pathology to outline open challenges and promising future research directions.

## II. OVERVIEW OF GENERATIVE PATHOLOGY

### A. Development timeline

The timeline of representative publications from 2017 to 2025 traces the evolution of generative modeling in computational pathology in Fig. 4. Early research focused on GAN-based image synthesis for stain normalization and patch-level data augmentation. Subsequent work broadened the scope of generative objectives, incorporating diverse architectures like Diffusion models and LLM/VLM for image synthesis, text generation, and multimodal generation. Recent

efforts emphasize generalist and foundation models with cross-modal generative capabilities, reflecting a trend toward scalable, data-driven frameworks that unify diverse generation tasks. The Sankey diagram in Fig. 5 illustrates the flow of generative tasks across inputs, model types, and outputs in pathology. Most models take image data as input, with outputs dominated by image and text. Diffusion models are most prevalent, followed by GANs, while LLMs and VLMs are emerging in text-based applications.

### B. Main Generative Method

In computational pathology, generative models have evolved into a diverse set of architectures, each offering distinct mechanisms for synthesizing data. The three primary classes of generative approaches include Generative Adversarial Networks (GANs), diffusion models, and their conditional frameworks. Fig. 6 illustrates representative architectures across these categories, offering a visual comparison of their generative mechanisms and structural differences.

1) *Generative Adversarial Network (GAN)*: GAN [8] represents a cornerstone methodology within generative modeling, employing a unique game-theoretic training paradigm. This framework involves two neural networks: a generator (G) tasked with synthesizing data samples intended to be indistinguishable from real data, and a discriminator (D) trained to differentiate between these real samples and the synthetic outputs from G. Their adversarial interplay is captured by the minimax objective function:

$$\min_G \max_D \mathbb{E}_{x \sim p_{\text{data}}} [\log D(x)] + \mathbb{E}_{z \sim p_z} [\log(1 - D(G(z)))], \quad (1)$$

where  $x$  denotes samples drawn from the real data distribution  $p_{\text{data}}$ , representing authentic pathology images, and  $z$  represents latent noise vectors sampled from a prior distribution  $p_z$ . The discriminator  $D(x)$  estimates the probability that  $x$  originates from the real data

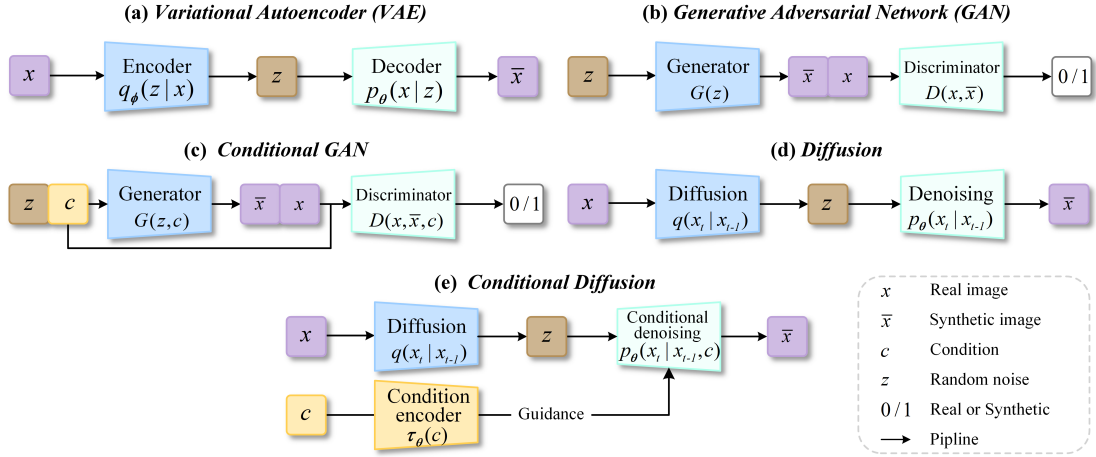


**Fig. 6.** A sketch of five representative generative model architectures. (a) VAE learns a probabilistic latent space and reconstructs images through encoder-decoder optimization. (b) GAN consists of a generator and a discriminator trained in a minimax game to produce realistic outputs. (c) Conditional GAN (cGAN) introduces external conditioning to guide the generation process. (d) The diffusion model performs iterative denoising to generate data by learning the reverse of a noise injection process. (e) Conditional Diffusion extends the diffusion framework with conditioning inputs to steer the generative trajectory during denoising.

distribution.  $D$  is optimized to maximize this objective (correctly identifying real vs. fake), whereas  $G$  is optimized to minimize it by generating increasingly realistic samples  $G(z)$  that deceive  $D$  (i.e., maximizing  $D(G(z))$ ). This adversarial process compels the generator to implicitly learn the complex underlying distribution of the training data, enabling the generation of high-fidelity samples.

GANs have become a cornerstone in computational pathology, addressing persistent challenges such as annotated data scarcity [9], class imbalance, and inter-institutional variability in staining and scanning protocols [10], [11]. By learning to approximate complex high-dimensional data distributions, GANs enable a spectrum of downstream applications including stain normalization, virtual staining, data augmentation, domain adaptation, and resolution enhancement. Among the most influential architectures is CycleGAN [12], which performs unpaired image-to-image translation using bidirectional generators and cycle-consistency constraints. GAN and its variants [13]–[15] have been widely applied in stain normalization [16]–[19], virtual staining [20], [21], artifact removal [22], and resolution enhancement [23]. Moreover, GAN discriminators have been utilized for unsupervised representation learning by capturing biologically meaningful features from histopathological images [24].

Conditional GANs extend this framework by enabling more controllable and semantically targeted generation. The Conditional GAN (cGAN) [25] introduces auxiliary label conditioning for class-specific synthesis, while Pix2Pix [26] enables paired image-to-image translation in a supervised setting. These models have been applied in generating lesion-specific features, modality-specific reconstructions, and cellular attribute-guided outputs. StyleGAN [27] advances latent space controllability through style-based modulation, supporting fine-grained synthesis aligned with clinical morphology. Notable applications include nuclei segmentation with morphologically guided augmentation [28], mitotic figure synthesis [29], rare class enhancement in prostate Gleason grading [30], and attribute- or lesion-guided generation for classification tasks [31]. Further innovations unify generation and prediction within a single framework [32], supporting integrated deployment in diagnostic pipelines.

**2) Diffusion Model:** Diffusion models [33] represent a major advancement in deep generative modeling, particularly excelling in high-fidelity image synthesis tasks [34], [35]. Denoising Diffusion Probabilistic Model (DDPM) [33] is the canonical example of diffu-

sion models that learns to synthesize data by reversing a predefined Markovian noising process. The process involves gradually corrupting data with Gaussian noise over a fixed number of steps, and learning a reverse denoising model to recover the original data distribution.

In the forward diffusion process, given an uncorrupted (original) data distribution  $q(x_0)$ , Gaussian noise is added to the original data  $x_0$  over  $T$  discrete time steps to obtain noisy latents  $\{x_t\}_{t=1}^T$ . This process is defined as:

$$q(x_t | x_0) = \mathcal{N}(x_t; \sqrt{\bar{\alpha}_t}x_0, (1 - \bar{\alpha}_t)\mathbf{I}), \quad (2)$$

where  $\mathcal{N}$  denotes the normal distribution,  $\mathbf{I}$  is the identity matrix, hyperparameter  $\{\beta_t\}_{t=1}^T \in [0, 1)$  represents the variance schedule across the diffusion steps,  $\alpha_t = 1 - \beta_t$ , and  $\bar{\alpha}_t = \prod_{s=1}^t \alpha_s$  is the cumulative product. A sample  $x_t$  from this distribution can be expressed as:

$$x_t = \sqrt{\bar{\alpha}_t}x_0 + \sqrt{1 - \bar{\alpha}_t}\epsilon, \epsilon \sim \mathcal{N}(0, \mathbf{I}). \quad (3)$$

The reverse denoising process learns a generative model that progressively removes noise from a prior distribution  $p(x_T) = \mathcal{N}(x_T; 0, \mathbf{I})$ , using a parameterized Markov chain:

$$p_\theta(x_{0:T}) = p(x_T) \prod_{t=1}^T p_\theta(x_{t-1} | x_t), \quad (4)$$

$$p_\theta(x_{t-1} | x_t) = \mathcal{N}(x_{t-1}; \mu_\theta(x_t, t), \Sigma_\theta(x_t, t)). \quad (5)$$

Equation (5) defines a Gaussian transition kernel where the neural network predicts the mean  $\mu_\theta(x_t, t)$  and covariance  $\Sigma_\theta(x_t, t)$  of the denoised distribution conditioned on the noisy input  $x_t$ .

To train the model, the objective is to maximize the data log-likelihood  $\log p_\theta(x_0)$ . However, since this quantity is intractable due to the marginalization over the latent variables  $x_{1:T}$ , a variational lower bound (VLB) is introduced following the evidence lower bound (ELBO) principle. The resulting objective decomposes into a sequence of Kullback–Leibler divergences (KL) and is given by:

$$\begin{aligned} \mathcal{L}_{\text{VLB}} = & -\log p_\theta(x_0 | x_1) + \text{KL}(p(x_T | x_0) \| \pi(x_T)) \\ & + \sum_{t=2}^T \text{KL}(p(x_{t-1} | x_t, x_0) \| p_\theta(x_{t-1} | x_t)), \end{aligned} \quad (6)$$

where  $\pi(x_T)$  denotes a fixed prior distribution, typically chosen as  $\mathcal{N}(0, \mathbf{I})$ , from which the reverse process is initialized. The variational

terms encourage the learned reverse transitions  $p_\theta(x_t|t)$  to approximate the true posteriors  $p(x_t|x_t, x_0)$  at each timestep. The simplified objective [33] is to train a model  $\epsilon_\theta(x_t, t)$  to predict  $\epsilon$  as follows:

$$\mathcal{L}_{\text{simple}} = \mathbb{E}_{t, x_0, \epsilon} \left[ \|\epsilon - \epsilon_\theta(x_t, t)\|^2 \right]. \quad (7)$$

Building upon the simplified noise prediction objective, subsequent frameworks such as Score-Based Generative Models (SGM) [36] and Score SDEs [37] extend diffusion modeling into continuous-time domains. These approaches formulate generation as a denoising process governed by learned reverse-time dynamics, allowing for improved flexibility in sampling and theoretical interpretability. Compared to the GAN-based methods, diffusion-based models offer more stable training behavior and exhibit strong resistance to mode collapse.

Diffusion models have become prominent tools in computational pathology due to their ability to generate high-fidelity synthetic images that preserve fine-grained tissue architecture and cellular morphology [38], [39]. They support diverse applications such as data augmentation for rare disease classes [40], [41], generation of gigapixel-scale whole-slide images [42], [43], and image quality restoration through denoising, artifact correction, and super-resolution [44], [45]. Additionally, diffusion frameworks enable flexible image-to-image translation, including stain normalization, virtual staining, and style transfer [46]–[48], facilitating cross-institutional harmonization and model generalization [49].

Conditional and controllable generation further expands the utility of diffusion models, enabling targeted applications through fine-grained synthesis control. Among the most widely adopted approaches are Classifier-Free Guidance (CFG) [50], Stable Diffusion [51], and ControlNet [52], each offering distinct conditioning mechanisms. CFG enables controllable generation in diffusion models by interpolating between conditional and unconditional predictions using a guidance scale during inference. Stable Diffusion performs generation in a compressed latent space conditioned on text, improving both efficiency and quality. ControlNet introduces trainable side networks to impose spatial constraints from inputs such as segmentation masks or edges while keeping the main model frozen. By conditioning on text descriptions [31], class labels [53], semantic maps, or specific lesions [54], researchers can generate specific cellular structures with corresponding labels [31], synthesize images reflecting specific mitotic figure characteristics [29], or even generate tumor WSI tiles conditioned on RNA-sequencing data [55]. This controllability extends to depicting pathological transitions [56] and creating counterfactual examples for model explainability [57]. While their iterative sampling process incurs computational cost, their precision and adaptability make them particularly suitable for tasks requiring anatomical coherence, visual realism, and semantic control.

**3) LLM/VLM:** Large language models and vision-language models have emerged as powerful generative tools in computational pathology, enabling cross-modal learning between histological images and diagnostic text. Rooted in Transformer architectures, VLMs such as CLIP [58], BERT [59], and ALIGN [60] leverage contrastive learning to align image and text embeddings, creating a shared representation space that supports both understanding and generation tasks across modalities. This alignment facilitates effective transfer learning from general-domain image–text pairs to data-scarce medical domains. Architectures like Flamingo [61] and BLIP [62] integrate pretrained large language components and refine pretraining objectives to support unified vision–language reasoning and generation.

Notably, it is important to distinguish LLMs and VLMs serving as generative models from those functioning primarily as foundation models for representation learning. As generative models, they are trained to model the data distribution  $p(x)$  or the conditional distribution

$p(x|c)$ , with the explicit goal of producing new, observable samples through a learned decoding process. Their training typically involves reconstruction-based, adversarial, variational, or denoising objectives, enabling tasks such as image synthesis, data augmentation, and cross-modal generation.

In computational pathology, domain-specific vision-language foundation models have been developed to address the complexity of histological image–text alignment. Models such as PathAlign [63] and C-CLIP [64] are pretrained on large-scale pathology image–report pairs using contrastive learning and cross-modal distillation strategies [65], [66]. These frameworks often incorporate hierarchical objectives and preprocessing pipelines tailored to pathology reports [67], enabling robust zero-shot and few-shot transfer to downstream tasks such as WSI classification and cancer subtype recognition [68]. Meanwhile, domain-adapted visual backbones like Hibou [69] further improve representation learning by embedding morphological priors directly into the visual encoder.

Beyond feature alignment, instruction-tuned multimodal assistants such as PA-LLaVA [70], SlideChat [71], and PathologyVLM [72] extend these models toward interactive clinical applications. By incorporating natural language instructions during fine-tuning [73], these systems support report generation, visual question answering, and text-guided interpretation, facilitating human–AI collaboration in diagnostic decision-making. These advances demonstrate a shift from static representation learning to generative, explainable, and task-adaptive VLMs tailored for pathology.

Current generative applications include image captioning, automated pathology report generation [74], and visual question answering [75]. While direct text-to-image synthesis in pathology remains underexplored compared to vision-only diffusion models, the robust multimodal representations learned by VLMs offer a strong foundation for future extensions. Furthermore, integration with genomic or clinical data has enabled models to support tasks such as outcome prediction [76], [77] and mitosis detection [78]. Continued efforts are needed to improve robustness, particularly under adversarial scenarios [79], and to extend controllable generative capabilities within multimodal frameworks.

**4) Other Generative Methods:** In addition to GANs, diffusion models, and vision-language models, other generative approaches such as variational autoencoders (VAE), autoregressive models, and reinforcement learning (RL)-based strategies have been applied in computational pathology. 1) VAEs provide a probabilistic framework for learning structured latent representations by jointly optimizing an encoder and decoder through the Evidence Lower Bound objective [80], [81]. Although VAEs tend to produce blurrier images than GANs or diffusion models [35], they offer advantages in learning smooth and interpretable latent spaces. In pathology, they have been used for self-supervised representation learning [82], feature-space augmentation to improve WSI classification [83], and conditional generation for imputing missing genomic profiles in multimodal survival prediction tasks [84]. 2) Autoregressive Models [85] define generation as a sequential process, modeling the probability of each data unit conditioned on previous ones. While achieving state-of-the-art performance in sequence modeling domains like natural language [86], their inherent sequentiality poses computational challenges for synthesizing high-resolution pathology images directly. Their principles, however, are fundamental to generating textual outputs related to pathology, such as clinical captions derived from WSIs to enhance downstream tasks like image retrieval [87]. 3) Reinforcement learning offers a policy-driven approach where generative outputs are optimized with respect to specific reward signals. Although not widely used for standalone image generation, RL has been integrated into generative pipelines for more precise control. It has been applied to

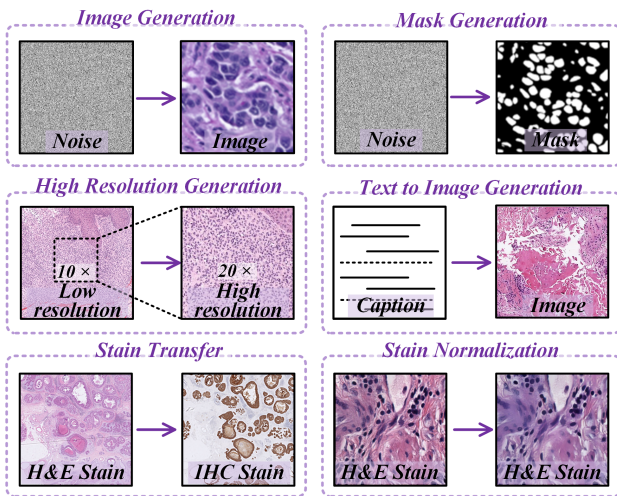


Fig. 7. Illustrative examples of image generation tasks demonstrating diverse input-output paradigms, including mask synthesis, resolution enhancement, text-to-image translation, and stain style transformation such as stain transfer and normalization.

enhance prompt-aligned synthesis [88], improve factual consistency in report generation [89], and reframe image enhancement tasks such as super-resolution as interpretable decision-making processes [90]. Overall, these generative frameworks complement dominant methods by offering unique strengths in latent modeling, sequential reasoning, and controllable generation, making them valuable components of the generative toolkit in computational pathology.

### III. GENERATION TASK

#### A. Image Generation

Image generation is a fundamental task in computational pathology that supports a wide spectrum of downstream applications by enriching data diversity, enhancing visual realism, and preserving domain-specific structures, as illustrated in Fig. 7. Recent advances in generative models have enabled the creation of high-fidelity synthetic images, addressing critical challenges such as limited labeled data, class imbalance, and domain shifts. In the context of pathology, image generation encompasses several sub-tasks with distinct goals: 1) synthetic image generation for data augmentation, which includes both conditional and unconditional generation paradigms; 2) mask generation, which emphasizes structural fidelity through the synthesis of corresponding segmentation masks; 3) high-resolution generation, which targets the production of multi-scale or even whole-slide images to meet clinical-resolution standards; and 4) text-to-image generation, which translates diagnostic descriptions or prompts into visual representations; and 5) stain style generation, including stain normalization and stain transfer.

##### 1) Synthetic Image/Augmentation:

a) *Conditional Image Generation:* Conditional generative models have become the mainstream approach for synthetic image generation in pathology, as they enable controllable synthesis guided by semantic labels, spatial priors, or biological attributes, thus better supporting downstream tasks such as segmentation, classification, and interpretability. Early works predominantly relied on GAN-based frameworks, where HistoGAN [91] synthesized image patches conditioned on class labels, introducing a selective augmentation mechanism that filters generated samples based on label confidence and feature similarity to real data. ProGleason-GAN [103] is a conditional progressive growing GAN framework for synthesizing prostate histopathology patches with controllable Gleason grades,

where grade-specific information is embedded into the generator to guide progressive image synthesis without modifying the adversarial loss. [32] proposed a unified ViT-based conditional GAN that simultaneously performs image synthesis and classification in a single-stage pipeline, tightly coupling generative and discriminative learning objectives for better feature alignment.

More recently, the field has witnessed a paradigm shift toward diffusion models, which offer superior visual fidelity, training stability, and flexibility in conditioning. Several works focus on feature-conditioned synthesis, such as ViT-DAE [101], which employs transformer-derived semantic features as conditioning inputs to guide DDIM sampling in the diffusion autoencoder. Moving beyond single-stage architectures, Nudiff [41] introduces a two-stage pipeline that first generates nuclei structure maps and then produces images conditioned on these structural priors, enhancing label-image alignment. Similarly, DiffMix [40] and USegMix [121] both leverage spatial semantic priors to guide diffusion-based image synthesis: DiffMix uses custom semantic maps with instance and class-type labels to generate balanced image-label pairs for improving segmentation in imbalanced datasets, while USegMix uses unsupervised SAM masks for realistic inpainting and tissue replacement, enhancing structural plausibility and diversity.

Beyond spatial and semantic conditioning, recent studies have further explored biologically grounded and structurally interpretable diffusion models that incorporate prior knowledge about disease progression, cellular morphology, and weak annotations. These approaches aim not only to generate visually realistic images but also to reflect meaningful biological variation or support clinically relevant tasks. For instance, Adaptive Depth-controlled Diffusion (ADD) [139] simulates the gradual transition between disease stages through a hybrid attention mechanism and a feature-aware depth controller, enabling soft-label image synthesis with consistent morphological progression across spatial regions. [29] proposes a mitosis-aware diffusion model that uses probabilistic mitotic scores as conditioning inputs, capturing the morphological continuum between non-mitotic and mitotic nuclei and enhancing interpretability in mitotic figure classification. [99] focuses on fine-grained conditioning by applying bell-shaped and reverse-sigmoid loss weightings to emphasize subtle spatial or molecular discriminative features, particularly in HPV-related OPSCC tissue synthesis. PDSeg [138] incorporates weak supervision by adapting ControlNet to binary control images and text prompts, avoiding the need for dense annotations. [39] enhances gland segmentation through multi-scale mask construction and feature-conditioned diffusion.

Conditional generation is also being explored for diagnostic or functional enhancement. For example, MoPaDi [140] enables counterfactual visual explanations by morphologically altering image patches to invert biomarker predictions, while AnoDDPM [108] detects out-of-distribution samples by reconstructing inputs under different noise conditions, offering a robust unsupervised anomaly detection strategy.

b) *Unconditional Image Generation:* While conditional generation has gained increasing attention, unconditional generative models remain a vital foundation for synthetic pathology image generation, especially in unsupervised settings or when annotations are limited. These methods primarily aim to model the overall distribution of pathology images, generating high-fidelity samples that enhance data diversity, support downstream tasks, or enable representation learning. GAN-based approaches have long served as a dominant paradigm, particularly for representation learning, semantic manipulation, and visual enhancement. PathologyGAN [141] pioneers phenotype-aware synthesis by learning an interpretable latent space structured by tissue-level phenotypes, enabling semantic vector op-

**TABLE I**  
OVERVIEW OF IMAGE GENERATION METHODS IN COMPUTATIONAL PATHOLOGY.

Year	Name	Input	Model	Output	Application Task
2017	SST [10]	Patch	GAN	Patch	Classification, Stain normalization
2018	[16]	Patch	GAN	Patch	Stain normalization
2020	[91]	Patch	GAN	Patch	Classification
2021	[92]	Patch	GAN	Patch	Segmentation, High resolution image
2021	Residual CycleGAN [93]	Patch	GAN	Patch	Segmentation
2021	PathologyGAN [94]	Patch	GAN	Patch	Classification, Generation
2021	PC-StainGAN [21]	Patch	GAN	Patch	Stain transfer, Image-to-image translation
2021	[17]	Patch	GAN	Patch	Classification, Stain normalization
2021	[82]	Patch	VAE	Patch	Classification, High resolution image generation
2021	Sharp-GAN [95]	Patch	GAN	Patch	Segmentation
2021	AttributeGAN [96]	Cellular attribute	GAN	Patch	/
2022	[97]	Patch	GAN	Patch	Segmentation
2022	MSSA-GAN [22]	Patch	GAN	Patch	Image restoration
2022	insMix [28]	Patch	GAN	Patch	Segmentation
2022	ProGAN [98]	Patch, WSI	GAN	Patch	Classification, Data augmentation
2022	[99]	Patch, HPV status	Diffusion	Patch	Classification, Image generation
2022	[100]	Patch	Diffusion	Patch	/
2022	[12]	Patch	GAN	Patch	Segmentation
2022	[49]	Patch	Diffusion	Patch	Classification, Segmentation
2023	[39]	Patch	Diffusion	Patch	Segmentation
2023	ViT-DAE [101]	Patch	Diffusion	Patch	Classification, Data augmentation
2023	Restore-GAN [23]	Patch	GAN	Patch	Classification, Segmentation, Detection
2023	SNOW [102]	Patch	GAN	Patch	Segmentation
2023	DiffMix [40]	Patch	Diffusion	Patch	Segmentation, Classification
2023	ProGleason-GAN [103]	Patch	GAN	Patch	Retrieval, Cancer grading
2023	ArtiFusion [104]	Patch	Diffusion	Patch	Classification
2023	[11]	Patch	GAN	Patch	Classification, Stain normalization
2023	[105]	Patch, Mask	Diffusion	Patch	Segmentation
2023	PathLDM [106]	Patch, Text	Diffusion	Patch	Image generation
2023	NASDM [38]	Patch, Mask	Diffusion	Patch	Segmentation, Image generation
2023	DiffInfinite [42]	Patch	Diffusion	Patch	Segmentation, Classification
2023	StainDiff [107]	Patch	Diffusion	Patch	Classification, Stain transfer
2023	[29]	Patch	Diffusion	Patch	Classification, Mitotic detection
2023	[43]	WSI	Diffusion	WSI	High resolution image
2024	[41]	Patch	Diffusion	Patch	Segmentation
2024	AnoDDPM [108]	Patch	Diffusion	Patch	Detection
2024	[109]	Patch	Diffusion	Patch	Detection
2024	[55]	Patch	GAN	Patch	Classification, Segmentation
2024	Diffusion-L [110]	Patch	Diffusion	Patch	Image-to-image translation, Uncertainty
2024	[111]	Patch	Diffusion	Patch	Classification, Image generation
2024	[18]	Patch	GAN	Patch	Classification
2024	ADD [56]	Patch	Diffusion	Patch	Classification
2024	StainDiffuser [46]	Patch	Diffusion	Patch	Report generation, Segmentation
2024	F2FLD [112]	Patch	Diffusion	Patch	Classification
2024	AV-GAN [113]	Patch	GAN	Patch	Image translation, Virtual staining
2024	DISC [53]	Patch	Diffusion	Patch	Classification, Cancer grading
2024	STAR-RL [90]	Patch	RL	Patch	High resolution image
2024	VIMs [114]	Patch, Text	Diffusion	Patch	Segmentation, Report generation
2024	ULSA [115]	Patch, WSI	GAN	Mask	Segmentation, Classification
2024	PathUp [116]	Patch, Text	Diffusion	Patch	Classification, High resolution image
2024	[44]	Patch	Other	Patch	Classification, Prognosis
2024	VirtualMultiplexer [117]	Patch	Other	Patch	Prognosis, Classification
2024	StainFuser [48]	Patch	Diffusion	Patch	Classification, Segmentation
2024	URCDM [118]	Patch	Diffusion	Patch, WSI	Image Synthesis
2024	Histo-Diffusion [119]	Patch	Diffusion	Patch	Classification
2024	TT-SaD [120]	Patch	Diffusion	Patch	Classification
2024	[31]	Text, Point maps	Diffusion	Patch	Segmentation, Classification
2024	USegMix [121]	Patch	Diffusion	Patch	Classification
2024	[32]	Patch	GAN	Patch	Classification, Image generation
2024	PST-Diff [122]	Patch	Diffusion	Patch	Image generation
2024	MDDP [123]	Patch	Diffusion	Patch	Classification, Image-to-image translation
2024	CC-WSI-Net [124]	Patch	GAN	Patch	Image generation, Classification
2024	MoPaDi [57]	Patch	Diffusion	Patch	Classification
2024	LatentArtiFusion [125]	Patch	Diffusion, VAE	Patch	Classification
2024	PPHM-GAN [20]	Patch	GAN	Patch	Detection, Classification
2024	STEDM [126]	Patch, Layout	Diffusion	Patch	Segmentation
2024	HADiff [127]	Patch	Diffusion	Mask	Segmentation
2024	[128]	Patch	Diffusion	Patch	Classification
2024	[129]	Patch	Diffusion	Patch	Classification, Synthetic data generation
2024	DUST [130]	Patch	Diffusion	Patch	Stain Transfer
2024	[131]	Patch	Diffusion	Patch	Detection, Classification
2025	[132]	Patch, Mask	Diffusion	Patch	Segmentation
2025	VM-GAN [133]	Patch	GAN	Patch	Image-to-image translation
2025	[134]	Patch, Mask	GAN	Patch	Segmentation, Data augmentation
2025	GenSelfDiff-HIS [135]	Patch	Diffusion	Mask	Segmentation
2025	DSTGAN [19]	Patch	GAN	Patch	Classification, Segmentation
2025	ToPoFM [136]	Patch	LLM/VLM	Patch	Classification, Segmentation
2025	PathoPainter [137]	Patch	Diffusion	Patch	Segmentation
2025	RBDM [47]	Patch	Diffusion	Patch	Report generation
2025	PDSeg [138]	Patch, Mask	Diffusion	Patch	Segmentation

erations and phenotype-aware image generation across cancer tissue types. [142] proposes a progressively grown adversarial autoencoder for self-supervised visual field expansion, which reconstructs large tissue regions from smaller input tiles while enforcing informative latent representations through dual discriminators and regularized objectives. For image restoration, MSSA-GAN [143] adopts a multi-scale self-attention generator to recover contaminated colon histology images by leveraging dependencies between corrupted and uncorrupted regions across scales. Notably, ProGleason-GAN [103] introduces weak conditioning into the GAN framework by embedding Gleason grade signals into the generator, enabling controlled prostate image synthesis without altering the adversarial loss, straddling the line between unconditional and soft-conditional generation. SNOW [102] introduces a large-scale synthetic pathological image dataset paired with the annotation for nuclei semantic segmentation through a standardized workflow by applying the off-the-shelf image generator and nuclei annotator based on StyleGAN2.

Unconditional diffusion models also have shown strong potential for synthesizing high-fidelity pathology images, particularly in addressing data scarcity and enhancing model robustness across domains. These methods commonly share the goal of enriching training datasets with realistic, label-free samples, but differ in their target modalities and the specific challenges they address. [100] explores diffusion probabilistic models for histopathology image synthesis, demonstrating superior visual quality and realism on brain cancer images by incorporating color normalization and perceptual morphology weighting. [144] targets deep ultraviolet fluorescence (DUV) breast cancer images, using patch-level diffusion synthesis to augment classification performance. [109] leverages diffusion models to generate synthetic images that address underrepresentation in training data, thereby enhancing the robustness and fairness of diagnostic models across diverse imaging modalities under domain shifts. While all three methods leverage the intrinsic advantages of diffusion models in achieving high visual fidelity, their focuses differ across stain-normalized refinement, modality-specific data augmentation, and fairness-driven sample balancing, which collectively demonstrate the versatility of unconditional diffusion models as a general-purpose framework for synthetic pathology image generation.

**2) Mask:** Mask-guided image generation has emerged as a crucial strategy for enabling structure-aware synthetic pathology images, supporting tasks such as data augmentation, segmentation training, and artifact correction. Depending on the generation targets, existing methods can be broadly categorized into three directions: Mask-to-Image generation, Joint Image-Mask generation, and Artifact Restoration via mask-guided synthesis. Within each group, diffusion-based models emphasize visual fidelity and structural consistency, whereas GAN-based models offer faster sampling and greater flexibility at the cost of slightly reduced image realism.

*a) Mask-to-image generation:* A major direction in mask-guided generation focuses on synthesizing realistic pathology images conditioned directly on segmentation masks or semantic maps. Diffusion-based methods dominate this category due to their superior fidelity and flexibility. [105] introduces a conditional diffusion model that synthesizes histopathology images from arbitrary segmentation masks, addressing class imbalance and enriching underrepresented structures. DISC [53] proposes a latent diffusion model with self-distillation from separated conditions, enabling accurate synthesis of prostate tiles conditioned on Gleason Grade masks and improving multi-grade representation. NASDM [38] refines semantic conditioning on multi-class nuclei masks based on denoising diffusion probabilistic models (DDPMs) for nuclei-aware semantic tissue generation. HADiff [127] advances coarse-to-fine mask-informed generation by extracting multi-resolution hierarchical features and

embedding auxiliary-generated priors into the diffusion process to enhance lesion structure preservation. On the GAN side, Sharp-GAN [95] enhances mask-to-image translation by replacing binary masks with normalized nucleus distance maps, introducing a sharpness loss to improve boundary resolution, particularly for overlapping nuclei. Compared to GAN-based approaches, diffusion models in this group generally achieve higher realism and better structural fidelity but are computationally more expensive.

*b) Joint image-mask generation:* Another line of research focuses on the simultaneous generation of both images and their corresponding masks, supporting fully paired data synthesis for segmentation model training. Diffusion-based approaches such as PathoPainter [137] perform mask-guided inpainting while incorporating tumor embedding sampling and uncertainty filtering, ensuring alignment between generated images and semantic masks. STEDM [126] proposes a conditional latent diffusion framework that synthesizes pathology images by jointly conditioning on predefined semantic layouts and extracted visual styles, leveraging a trainable style encoder and a multi-style aggregation module to enable zero-shot image-mask pair generation across unseen styles. [132] adapt appearance transfer techniques to diffusion models, using cross-image attention and class-specific information to guide mask-to-image generation, thereby preserving realistic morphological structures in immunohistochemistry (IHC)-stained images. DiffInfinite [42] further advances this direction by introducing a hierarchical two-stage diffusion framework that first generates scalable coarse segmentation masks from high-level prompts and then synthesizes high-fidelity histological images through patch-based diffusion conditioned on those masks. This architecture enables artifact-free image assembly at arbitrary scales and supports semi-supervised learning, making it suitable for privacy-preserving and data-efficient augmentation. On the GAN side, several methods explore more efficient and controllable pathways for mask-guided image synthesis. Pathopix-GAN [134] adopts a GAN-inspired architecture that synthesizes histopathology patches and their semantic masks through semantically adaptive normalization, facilitating effective data augmentation. AttributeGAN [96] enables fine-grained control over cellular features by conditioning generation on specific attributes such as cell crowding, polarity, mitotic activity, nucleolar prominence, and nuclear pleomorphism. It employs attention mechanisms and conditional contrastive learning to enhance both image fidelity and biological interpretability. While diffusion models excel at capturing global coherence and supporting zero-shot style transfer, GAN-based approaches offer greater computational efficiency, latent space controllability, and targeted conditioning, making them well-suited for large-scale segmentation augmentation.

*c) Artifact Restoration:* Beyond segmentation-related generation, mask-guided diffusion has also been explored for artifact restoration. LatentArtiFusion [125] proposes a latent diffusion-based framework for histological artifact restoration that performs selective regional denoising in a low-dimensional latent space guided by artifact masks, enabling efficient and high-fidelity reconstruction of corrupted regions while preserving non-artifact tissue context.

**3) Multi/High Resolution:** Despite recent advances, generating high-fidelity pathology images at high and multiple resolutions remains a significant challenge. In particular, synthesizing images that simultaneously preserve fine-grained spatial details at a single scale and maintain anatomical consistency across multiple magnifications is critical for realistic pathology modeling but remains difficult to achieve. Recent works are broadly divided into high-resolution and multi-resolution synthesis approaches.

*a) High Resolution Generation:* High-resolution generation focuses on synthesizing pathology images with extremely fine spatial details at a single target scale, often for improving diagnostic utility

or classifier robustness. Early work by [98] applied a progressive GAN framework to generate  $1024 \times 1024$  pathology patches across ten histotypes, showing perceptual realism and effective augmentation benefits. Extending to larger fields, ToPoFM [136] combines topology-informed cell arrangement generation with latent diffusion to synthesize  $2048 \times 2048$  images, achieving cellular-level spatial control. Moving to gigapixel-level WSI synthesis, [43] introduces a coarse-to-fine sampling strategy within a diffusion framework to generate WSIs as large as  $65536 \times 65536$  pixels, which sequentially adds fine details to increase the resolution. Similarly, URCDMs [118] proposes a cascaded conditional diffusion architecture that generates WSIs with over  $10^9$  pixels by progressively synthesizing across hierarchical magnification levels while maintaining spatial coherence and anatomical fidelity.

*b) Multi-resolution Generation:* Recent work on multi-resolution pathology image generation focuses on improving fidelity, semantic consistency, and scale adaptiveness across magnifications. Histo-Diffusion [119] introduces a dual-stage conditional diffusion framework that first restores histological priors and then applies controllable super-resolution, with evaluation guided by both full- and no-reference image quality metrics. Building on structural alignment, PathUp [116] synthesizes multi-resolution, multi-class images by combining patch-wise timestep tracking to mitigate tiling artifacts and a patho-align module that injects expert priors, while feature entropy loss promotes inter-class diversity. STAR-RL [145] reformulates super-resolution as a spatial-temporal hierarchical reinforcement learning problem, where a spatial manager identifies low-quality regions, a temporal manager decides when to terminate restoration, and a pixel-level agent performs sequential enhancement. This design enables adaptive, region-aware reconstruction with improved efficiency and interpretability. [129] proposes a class-conditioned diffusion model guided by patch size and label prompts to synthesize images across varying fields of view from  $64 \times 64$  to  $224 \times 224$ . By explicitly encoding spatial scale into the generative process, the model supports scale-aware representation learning and improves classification robustness under resolution shifts.

Overall, high-resolution methods support detailed image synthesis for both localized tissue analysis and ultra-large-scale whole slide images, while multi-resolution approaches aim to ensure semantic and structural consistency across magnifications. As both directions advance, integrating adaptive resolution control with scalable WSI generation represents a promising pathway toward unified and diagnostically robust synthetic pathology frameworks.

*4) Text to Image:* Text-to-image generation in pathology aims to bridge linguistic clinical descriptions and visual tissue synthesis, enabling controllable and semantically rich image generation. PathLDM [106] introduces a text-conditioned latent diffusion model tailored for histopathology, leveraging GPT-3.5 to summarize diagnostic reports and integrate contextual textual cues into the image generation process. In parallel, VIMs [114] develops a text-to-stain diffusion framework that synthesizes IHC markers from H&E-stained (Hematoxylin and Eosin) images using textual prompts, requiring only uniplex IHC training data. Consequently, language-driven generative models hold significant promise for interpretability, modality translation, and report-informed synthesis in digital pathology.

#### *5) Stain:*

*a) Stain normalization:* The inherent variability in histological staining across laboratories, protocols, and equipment presents a major obstacle to the development of generalizable computational pathology algorithms. While traditional color normalization techniques offer partial solutions, the rise of deep generative models has enabled sophisticated data-driven approaches to standardize stain appearances, primarily within the ubiquitous H&E stain, thereby

enhancing the robustness of downstream analysis.

GANs are quickly used for unsupervised stain normalization due to their image-to-image translation capabilities. Researchers are exploring GAN-based and non-GAN-based methods to address visual variability in digital pathology images [18], aiming to improve AI model robustness and generalizability. CycleGAN emerges as a key tool [17], effectively mapping H&E images between domains, significantly improving downstream classification when test data was normalized to the training domain, validating GAN-based standardization for datasets with stain variations. ULSA [115] combines conditional GAN-based stain translation and stain-invariant feature consistency learning for semi-supervised training. The limited structural fidelity and controllability of basic GANs and CycleGANs have prompted the development of more advanced generative architectures.

To address the structural degradation often observed in standard CycleGAN-based normalization, [93] proposes Residual CycleGAN, which introduces a global skip connection to isolate stain differences while preserving morphological content. This design enables the generator to focus on learning residual stain transformations, resulting in improved robustness and a 9–10% gain in Dice segmentation accuracy on external datasets, particularly under low-data regimes. Extending this direction, [146] develops DSTGAN, which leverages a Swin Transformer backbone to capture long-range contextual information and incorporates deep supervision along with a semi-supervised training scheme, collectively achieving state-of-the-art performance in stain normalization. For more explicit disentanglement of visual attributes, [16] introduces an InfoGAN-inspired approach that decouples structural content from color characteristics using latent variables. This framework enables stain normalization toward a target template while avoiding assumptions about tissue type or batch-dependent statistics.

To better align stain normalization with downstream tasks, the Neural Stain-Style Transfer (SST) network was proposed [10]. By introducing a feature-preserving loss, SST encourages normalized images to retain latent features aligned with the target domain, thereby directly optimizing for improved classification performance. To address the scarcity of paired training data, StainFuser applies neural style transfer to generate modified source–target image pairs, enabling the construction of the large-scale SPI-2M dataset [48].

To address data privacy in multi-institutional studies, a federated learning system is designed to expand normalization [11]. It used a federated cGAN with decentralized discriminators and temporal self-distillation, achieving privacy-preserving stain normalization and a 20% classification accuracy improvement. Diffusion models have emerged as alternatives to GANs for stain normalization. [147] applied score-based diffusion models (SBDM) to H&E normalization, using stain separation (SNMF) and patching to mitigate challenges in large WSIs. [120] introduced Test-Time Stain Adaptation using Diffusion (TT-SaD), formulating stain shift as an inverse problem solved during inference, enhancing classifier robustness without retraining. While focusing on generative normalization, related techniques address broader image quality. Restore-GAN [148] targets deblurring and super-resolution using a GAN framework, with an optional color normalization variant using traditional H&E deconvolution, illustrating the potential for multi-task generative quality enhancement.

Recent advances have shifted toward diffusion models, which offer improved generation fidelity, uncertainty modeling, and training stability. Conditional Denoising Diffusion Models (DDMs) have been applied to autofluorescence-to-H&E translation [149], and polarimetric Mueller Matrix data have been virtually stained using RBDM with tailored physical constraints [47]. To enhance structural consistency, training-free frameworks such as DDIM inversion with dual-path prompting [131], and PST-Diff [122] with pathological constraints

have been introduced. Models like StainDiffuser [46] and DUST [150] demonstrate diffusion’s flexibility in multi-task and multi-stain generation within unified architectures. Moreover, virtual staining has been integrated into representation learning. For instance, Lou et al. [123] use H&E-to-IHC translation as a pretext task within a contrastive learning framework, improving feature extraction and downstream WSI classification.

b) *Stain Transfer*: Stain transfer and virtual staining aim to computationally predict one staining modality from another, offering non-destructive, standardized alternatives to traditional histological staining. Unlike stain normalization, which harmonizes existing stain variations, virtual staining synthesizes entirely new stain representations, enabling applications such as label-free diagnostics, multiplexed analysis, and data augmentation.

Early approaches predominantly employed GANs, particularly CycleGAN variants, for unpaired image-to-image translation. However, issues such as tiling artifacts, structural distortion, and insufficient semantic control limited their clinical reliability. PC-StainGAN [21] introduces pathology consistency constraints via Pathological Representation Networks (PRNs) and structural similarity (SSIM) loss to enhance semantic mapping and structural fidelity in H&E-to-Ki-67 translation. For WSI virtual staining, CC-WSI-Net [124] proposes a GAN-based framework for virtual IHC staining that synthesizes seamless whole slide images from HE-stained inputs by introducing content and color consistency modules to mitigate tile-boundary artifacts and ensure accurate stain translation across the entire WSI. CycleGAN-PEC [92] addresses this with a perceptual embedding consistency (PEC) loss, enforcing semantic consistency across tiles. VM-GAN [133] proposes a value mapping constraint and confidence tiling to mitigate GAN instability and tiling artifacts, showing superior performance without task-specific tuning. Addressing staining unreliability in CycleGANs, the VirtualMultiplexer [117] uses a generative toolkit inspired by contrastive unpaired translation (CUT), maximizing mutual information between domains to preserve content accurately. The variability in tissue structure and staining intensity within samples presents another challenge. [113] addresses this with the Attention-Based Varifocal Generative Adversarial Network (AVGAN), using attention and a varifocal module for multi-resolution processing, improving performance in virtual kidney tissue staining. Extending GANs to handle multi-stain transformations within a single framework is crucial, and PPHM-GAN [20] addressed high-resolution any-to-any translation between multiple stains.

Recent advances in computational pathology have increasingly focused on diffusion models, which offer significant advantages in terms of generation fidelity, uncertainty modeling, and training stability. [149] introduces conditional Denoising Diffusion Models (DDMs) for translating autofluorescence (AF) images into virtual H&E stains, proposing a perceptual metric (Frechet StainNet Distance, FSD) and exploiting the inherent stochasticity of diffusion processes for uncertainty quantification. Extending the scope of diffusion-based virtual staining, RBDM [47] presents the first framework for converting label-free polarimetric Mueller Matrix (MM) images into virtual stains, incorporating fidelity-aware constraints to enable non-destructive tissue analysis. To improve structural stability and domain consistency during translation, [131] develops a training-free approach that leverages DDIM inversion with a Dual Path Prompted Strategy for unpaired multi-domain stain transfer. Similarly, PST-Diff [122] enforces Pathological and Structural Consistency Constraints to enable robust H&E-to-IHC transformations. Moreover, the flexibility of diffusion models has also facilitated multi-task learning frameworks. StainDiffuser [46] performs simultaneous virtual staining and target cell segmentation through dual diffusion pathways, while DUST [150] introduces a unified architecture capable of

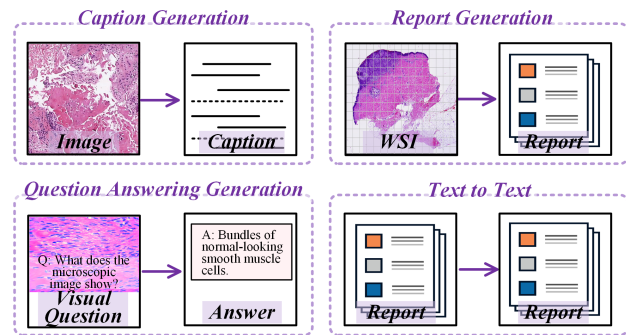


Fig. 8. Illustrative examples of text generation tasks, including text-to-text generation, patch-level image captioning, WSI to report generation, and text synthesis from image–text pairs.

any-to-any stain conversion within a single model. Beyond direct stain synthesis, diffusion models have been applied to representation learning. [123] proposes a diffusion-based pretraining pipeline that combines H&E-to-IHC translation with contrastive learning to derive semantically enriched representations from H&E patches, thereby enhancing downstream performance in WSI classification tasks.

The progression from GAN-based approaches to diffusion-based frameworks represents a fundamental shift in virtual staining, driven by the need for enhanced structural fidelity, cross-domain generalization, and clinical reliability. While challenges related to computational overhead and regulatory approval remain, diffusion models hold significant promise for transitioning virtual staining from experimental research into clinical practice. Future efforts should focus on developing efficient, interpretable, and scalable architectures, rigorously validated across diverse, multi-institutional datasets and seamlessly integrated into digital pathology workflows.

## B. Text Generation

Text generation in computational pathology encompasses a range of tasks that facilitate semantic interpretation, clinical communication, and automated reasoning. These include: 1) caption or description generation at the patch or cell level, 2) question answering, 3) report generation, and 4) text-to-text generation tasks such as automated information extraction and dialog-based interaction. Representative examples of these tasks are illustrated in Fig. 8.

1) *Caption/Description*: The ability to automatically generate precise and relevant descriptions for pathology images is crucial for enhancing diagnostic processes and supporting clinical decisions. Automatically describing pathology images presents unique challenges, such as the computational complexity arising from the gigapixel resolution of WSIs, the necessity to capture subtle cytological and histological features, and the high demand for clinical terminology accuracy. In this section, we explore recent research efforts aimed at improving captioning techniques in pathology, highlighting key methodologies and findings from several studies.

To refine the quality of generated descriptions, researchers have developed hybrid architectural models. Multiple Instance Learning (MIL) has been adapted for captioning tasks. [151] introduces the ARCH dataset, featuring dense image captions from pathology textbooks and articles, facilitating CP tasks through dense supervision. The dataset enables models to generate captions via implicit supervision, learning from image region relationships. Furthermore, the paper employs a hybrid architecture of Multi-Task Learning (MTL) and Multiple Instance Captioning (MIC), sharing a ResNet-18 encoder between a transformer decoder (for caption data learning) and linear decoders (for performing other tasks). MIL enhances visual

TABLE II

OVERVIEW OF TEXT GENERATION METHODS IN COMPUTATIONAL PATHOLOGY, DETAILING INPUT TYPES, MODEL ARCHITECTURES, GENERATED OUTPUTS, AND APPLICATION TASKS.

Year	Name	Input	Model	Output	Application Task
2021	[151]	Patch	Other	Text	Classification, Report generation, Image captioning
2023	TraP-VQA [75]	Patch, Text	LLM/VLM	Text	VQA
2023	LLaVA-Med [152]	Patch, Text	LLM/VLM	Text	VQA
2023	SGMT [153]	Patch, WSI	ViT	Text	Report generation
2023	QUILT-LLAVA [154]	Patch, WSI	LLM/VLM	Text	Report Generation, VQA
2023	[74]	WSI	LLM/VLM	Report	Report generation, Classification
2024	HistoGPT [155]	WSI	LLM/VLM	Report	Report generation
2024	HistGen [156]	WSI, Report	ViT	Report	Report generation
2024	BLIP [78]	Patch	LLM/VLM	Text	Detection
2024	MI-Gen [157]	WSI	LLM/VLM	Report	Report generation
2024	PathGen-CLIP [158]	Patch	LLM/VLM	Text	Classification, Report generation
2024	PathAlign [63]	WSI, Report	LLM/VLM	Report	Report generation, Retrieval, Classification
2024	CPLIP [64]	Patch, Text	LLM/VLM	Text	Classification, Retrieval
2024	PathChat [159]	Patch, Text	LLM/VLM	Text	Report generation, VQA
2024	PathM3 [160]	WSI, Text	LLM/VLM	Text	Classification, Report generation
2024	CLOVER [73]	Patch, Text	LLM/VLM	Text	Detection, VQA
2024	PathInsight [161]	Patch, Text	LLM/VLM	Report	Classification, Report generation, VQA
2024	PA-LLaVA [70]	Patch, Text	LLM/VLM	Text	VQA, Report generation
2024	[162]	Patch	LLM/VLM	Text	Image Captioning, Report generation
2024	W2T [163]	WSI, Text	LLM/VLM	Text	VQA, Classification, Prognosis
2024	SlideChat [71]	WSI	LLM/VLM	Text	Report generation, VQA
2025	PolyPath [164]	WSI, Report	LLM/VLM	Report	Report generation
2025	[165]	WSI, Report	LLM/VLM	Report	Report generation, Retrieval
2025	KR-MLFS [166]	WSI	LLM/VLM	Report	Report generation
2025	PathFinder [167]	WSI, Text	Agent	Report	Classification, Report generation
2025	PathologyVLM [72]	Patch, Text	LLM/VLM	Text	VQA, Report generation
2025	[168]	Report	LLM/VLM	Report	Prognosis, Classification

context understanding, improving the generated descriptions. On the other hand, [169] proposes an Enhanced Descriptive Captioning Model that integrates convolutional neural networks (CNNs) with advanced language models, focusing specifically on histopathological images. This multi-stage approach begins with feature extraction via CNNs, followed by the generation of coherent and detailed captions through recurrent neural networks (RNNs) or transformers, thereby providing a nuanced understanding of the visual content. [97] introduces the automated diagnostic caption generation from gastric adenocarcinoma biopsy patches, using a CNN encoder with pre-trained feature extractors and an attention-based RNN decoder trained to sequentially generate text from patch-level features.

Recent advancements in multimodal large language models have improved the interpretation of pathology images, particularly in generating captions for gigapixel WSIs. A prominent example is the subtype-guided Masked Transformer (SGMT) [153], which processes WSIs as sequences of sparse patches to reduce computational load while utilizing an Asymmetric Masked Mechanism. This model integrates a subtype prediction task during training to ensure that generated captions include both descriptive and clinically relevant information. This methodology demonstrates significant improvements over traditional RNN-based approaches on gastric adenocarcinoma datasets, highlighting the effectiveness of guided Transformer architectures in producing relevant captions for pathological images. PathM3 [160] serves as a prominent framework within this landscape, employing a multimodal, multi-task, and multiple instance learning strategy to effectively align gigapixel WSIs with limited diagnostic captions. By utilizing a query-based transformer similar to BLIP-2 and incorporating an MIL aggregation module, PathM3 enhances the robustness of caption generation. This method optimizes the use of available data, achieving significant improvements in the accuracy and relevance of diagnostic captions compared to baseline approaches. HistGen [156] proposes histopathology report generation, featuring a local-global hierarchical encoder for aggregating whole slide image features and a cross-modal context module for aligning visual and textual modalities, achieving state-of-the-art performance

on report generation, cancer subtyping, and survival analysis.

In addition to these advancements, the exploration of in-context learning presents a promising avenue for enhancing the generation of captions in pathology image analysis. [162] demonstrates that in-context learning with GPT-4V effectively classifies and describes cancer pathology images with minimal prompting. By framing prompts with few-shot examples, the model articulates essential features, highlighting its potential for generating concise and contextually accurate descriptions. This study illustrates that large vision-language models, even when trained on non-domain-specific data, can be effectively applied to pathology image processing tasks in histopathology, thereby expanding the toolkit available for automated image caption and description.

**2) Question Answering:** Visual Question Answering holds significant promise for computational pathology, offering a means to extract critical information from the vast landscape of WSIs and thereby enhance diagnostic efficiency and accuracy. Recognizing this potential, recent efforts have focused on developing models for VQA, such as PathChat [159], a general-purpose multimodal AI assistant, which integrates a vision encoder with a large language model to process and respond to both visual and textual inputs. This part synthesizes recent advancements in pathology VQA, focusing on model architectures, interpretability techniques, and clinical applications, while also addressing existing challenges and outlining future research trajectories.

Patch-level pre-training limits the application of multimodal large language models to pathology, hindering slide-level tasks. To address this, [163] introduces the WSI-VQA framework with a Wsi2Text Transformer (W2T) model, enabling pathologists to interactively interpret WSIs. [71] tackles the patch-level limitation issue with SlideChat, an open-source vision-language assistant utilizing hierarchical processing and trained on the SlideInstruction dataset. Addressing the lack of spatially-grounded capability for WSI analysis, [154] introduces QUILT-INSTRUCT, and trains QUILT-LLAVA, a multimodal model that reasons beyond single image patches. Beyond enabling WSI-level vision in VQA, interpretability is paramount.

[75] develops TraP-VQA, integrating ResNet50 and BioELMo with multimodal attention, providing interpretable responses and achieving 64.82% accuracy on PathVQA [170]. TraP-VQA employs visualization techniques like Grad-CAM to highlight relevant areas. Addressing computational costs, [73] presents a framework leveraging GPT-3.5-generated instructions and template-based pairings to achieve high accuracy with fewer parameters.

Despite progress, pathology VQA faces challenges including data scarcity, limited generalization, and the lack of clinical implementation. Future research should prioritize multimodal data fusion, transfer learning, and explainable AI. Rigorous clinical validation is needed to assess real-world impact, alongside standardization and interoperability for broader adoption.

**3) Report:** Pathology report generation is a crucial aspect of modern medical diagnosis, transforming complex visual information, such as whole slide images, into structured and comprehensive textual descriptions. This provides key evidence for disease diagnosis, prognosis assessment, and treatment planning [155], [166]. However, automatically generating high-quality, clinical-grade pathology reports presents several challenges, including handling high-resolution images, incorporating domain expertise, and balancing global and local information.

The rapid advancement of multimodal large models spurs increased attention toward domain-specific knowledge and capabilities within the medical field. HistoGPT [171], the first vision-language model for multi-image pathology report generation, is trained on over 15,000 WSIs and corresponding reports from dermatology patients, and demonstrates human-level reporting quality, zero-shot generalization to tumor subtyping and thickness prediction, and strong cross-cohort transferability across diverse geographic datasets. [161] fine-tunes multimodal large models such as LLaVA and Qwen-VL using a curated dataset of approximately 45,000 cases (PathEnhanceDS), significantly improving instruction-following performance. For a specific clinical task, [165] develops a vision-language model using a Contrastive Captioner framework, trained on 42,512 images and 19,645 reports of melanocytic lesions, to automate pathology report generation. The study concludes that model-generated reports for common nevi are comparable to pathologist-written ones, showing promise for workload reduction, while cross-modal retrieval proves more effective for rarer subtypes.

One of the key challenges in pathology report generation lies in the effective fusion of high-resolution images and textual modalities. Sengupta & Brown [74] address this by leveraging powerful pre-trained Transformer models to encode WSIs and automatically generate pathology-specific reports through an end-to-end training mechanism. Notably, their findings suggest that domain-specific initialization of the language modeling decoder does not offer significant performance gains, reinforcing the idea that domain-specific fine-tuning yields better results than pre-trained weight initialization.

Due to the gigapixel size of WSIs, balancing global context and local key regions presents another major challenge. [155] tackles this with HistoGPT, trained on WSIs and corresponding pathology reports. By extracting WSI features using pre-trained vision models and generating reports with a Transformer architecture, along with a novel visual prompt tuning strategy and a dual contrastive learning objective, HistoGPT outperforms existing methods in generating clinical-grade pathology reports. [157] proposes a multiple instance generation model (MI-Gen) by incorporating a hierarchical position-aware module in the Transformer encoder to enhance the model's spatial information perception in WSIs. [166] combines knowledge retrieval and multi-level regional feature selection, using a multi-level regional feature selection network and a knowledge retrieval decoder to assist report generation.

Pathology reports necessitate highlighting critical findings at the patch level within WSIs and integrating interpretations from multiple slides. To address the difficulty of creating robust image-text pairs, [63] develops PathAlign, learning slide-level visual-language alignment by pairing WSIs with corresponding diagnostic text from pathology reports. They further extend their work to multiple high-magnification regions across multiple WSIs [164], leveraging LoRA to fine-tune Gemini 1.5 Flash, generating part-level reports. Expert pathologist evaluations indicate that the generated report text is clinically accurate, with a high percentage exhibiting no clinically significant errors or omissions. With traditional AI methods failing to replicate the holistic, iterative diagnostic process of pathologists, [167] introduces PathFinder, a multimodal, multi-agent AI framework with Triage, Navigation, Description, and Diagnosis agents that collaboratively analyze WSIs, generating natural language explanations for its findings. PathFinder significantly outperforms existing methods and human pathologists in melanoma diagnosis, offering a new standard for accurate and interpretable AI-assisted pathology

Overall, the field of pathology report generation has transitioned from exploring general-purpose models to focusing on multimodal fusion and domain adaptation, demonstrating significant progress in handling high-resolution images, balancing global-local information, and integrating multi-slide data. Future research will likely emphasize finer-grained knowledge integration and clinically oriented optimization to bridge the gap between research and practical application.

**4) Text to text:** The application of LLMs in pathology is rapidly transforming how we handle textual data, with promising advancements in both information extraction and patient communication. Several recent studies highlight the potential of generative AI to streamline workflows and improve healthcare outcomes.

One key area is the automation of structured information extraction from unstructured pathology reports. A study leveraging ChatGPT demonstrates highly accurate extraction and structuring of data from breast cancer pathology reports [181], significantly reducing processing time. Similarly, research evaluating GPT-4o and Llama 3 shows that LLMs can achieve extraction accuracy comparable to trained human annotators [182], paving the way for open-source tools that enhance data accessibility and interoperability for clinical research. Further extending these applications to more complex analytical tasks, [168] evaluates LLMs, including the GPT family, Mistral, and Llama models, for their performance in cancer type identification, AJCC stage determination, and prognosis assessment from pathology reports. Based on this evaluation, two instruction-tuned models, Path-llama3.1-8B and Path-GPT-4o-mini-FT, are developed, demonstrating superior zero-shot performance in these critical pathology tasks. These advancements address the long-standing challenge of manually converting unstructured text into structured data, a process that is both time-consuming and error-prone.

Beyond structured data extraction, large language models (LLMs) also show considerable promise in enhancing doctor-patient communication. Recent studies employing GPT-4 to generate interpretive pathology reports (IPRs) have demonstrated improved readability and patient comprehension, while simultaneously reducing communication time between clinicians and patients [183]. The high alignment between LLM-generated IPRs and original clinical reports further underscores their potential to bridge the communication gap and support informed patient engagement. However, existing evaluations are often constrained to specific cancer types or single-institution datasets, highlighting the need for broader validation across diverse clinical settings. Despite these limitations, current evidence suggests that LLMs have the potential to transform pathology workflows by supporting both automation and clinician-patient communication, ultimately enhancing diagnostic efficiency and patient-centered care.

TABLE III

OVERVIEW OF MULTIMODAL GENERATION METHODS IN COMPUTATIONAL PATHOLOGY, DETAILING INPUT TYPES, MODEL ARCHITECTURES, GENERATED OUTPUTS, AND APPLICATION TASKS.

Year	Name	Input	Model	Output	Application Task
2023	Med-PaLM M [172]	Patch, Text, Gene	LLM/VLM	Multiple modality	Classification, Report generation, VQA
2024	CONCH [173]	Patch, WSI, Text	LLM/VLM	Multiple modality	Classification, Segmentation, Retrieval, Cancer grading
2024	PathAsst [174]	Patch, Text	LLM/VLM	Multiple modality	Report generation, Classification, Detection, Segmentation, Biomarker prediction, Retrieval, VQA
2024	PRISM [175]	WSI, Report	LLM/VLM	Multiple modality	Classification, Detection, Report generation, Biomarker prediction
2024	SongCi [176]	WSI, Text	LLM/VLM	Multiple modality	Classification, Report generation, Segmentation
2024	GPFM [177]	Patch, Knowledge	LLM/VLM	Multiple modality	Classification, Prognosis, Report generation, Biomarker prediction, Mutation prediction
2024	mSTAR [178]	WSI, Reports, Gene	Other	Multiple modality	Prognosis, Classification, Biomarker Prediction
2024	MUSK [76]	WSI, Text	LLM/VLM	Multiple modality	Prognosis, Biomarker prediction
2024	PathoDuet [179]	Patch, WSI	ViT	Multiple modality	Classification, Detection, Prognosis, Biomarker prediction
2025	PathOrchestra [180]	Patch, WSI	ViT	Multiple modality	Classification, Detection, Segmentation, Biomarker Prediction, Report generation

### C. Multimodal Generation

Multimodal generation in computational pathology aims to integrate histology images, clinical text, and molecular data into unified models that produce diagnostically meaningful outputs such as reports, visual responses, or synthetic representations. Current approaches can be broadly categorized as fully generative, generation-supportive, or representation-based with generative extensions.

*a) Fully Generative Models:* Fully generative models incorporate explicit decoding mechanisms to perform cross-modal generation, often producing natural language outputs from visual or multimodal inputs. Med-PaLM M [172] represents one of the first general-purpose biomedical foundation models capable of performing open-ended generation across a wide range of clinical tasks. The model is built on a unified encoder-decoder transformer architecture, jointly pretrained across text, radiology, dermatology, pathology, and genomics. It leverages multitask instruction tuning and modality alignment via tokenized input formatting, enabling tasks such as visual question answering, summarization, classification, and report generation. Evaluated on 14 benchmark tasks from the MultiMed-Bench suite, the model demonstrates strong zero-shot and cross-domain transfer capabilities. PRISM [175] is a slide-level generative model trained on 500,000 WSIs and 195,000 clinical reports. It aggregates tile-level embeddings into slide-level representations using attention pooling, followed by contrastive and generative pretraining. Generation is performed via a BioGPT-based transformer decoder with cross-attention, enabling free-text report generation, biomarker prediction, and zero-shot classification. mSTAR [178] is a multimodal foundation model for computational pathology that integrates H&E whole-slide images, pathology reports, and RNA-Seq profiles through a two-stage pretraining strategy combining slide-level contrastive learning and patch-level self-taught training. It is trained on 26,169 slide-level samples from 10,275 patients across 32 cancer types. mSTAR achieves strong performance across 43 downstream tasks and supports report generation from WSIs, reflecting both multimodal alignment and generative capabilities at the slide level. CONCH [173] adopts a Contrastive Captioning (CoCa) framework comprising an image encoder, a text encoder, and a multimodal transformer decoder. Pretrained on 1.17 million image-captions pairs using both contrastive alignment and captioning loss, it enables image-to-text generation, such as slide captioning and text-to-image retrieval, achieving state-of-the-art performance across 14 benchmarks involving classification, segmentation, retrieval, and generation. SongCi [176] is a vision-language model developed for forensic pathology, trained on 16 million histopathology patches, 2,228 WSI-text pairs, and 471 structured diagnoses. It integrates prototypical contrastive learning, cross-modal alignment, and diffusion-based generation to support zero-shot forensic diagnosis, interpretable text generation,

and patch synthesis conditioned on visual-language prototypes.

*b) Generation-Supportive Multimodal Models:* These models focus primarily on learning joint visual-textual representations through contrastive or masked modeling, while supporting limited generative tasks such as structured report generation or captioning. PathOrchestra [180] is trained on 27,755 WSIs and 9.4 million regions of interest using a combination of contrastive learning and weak supervision. It aggregates region-level features to slide-level representations and is evaluated on 112 downstream tasks, including cancer classification, biomarker prediction, and gene expression estimation. Notably, it enables structured report generation for colorectal cancer and lymphoma by combining H&E and IHC-based predictions, demonstrating scalable clinical utility with partial generative capability. MUSK [76] proposes a multimodal masked transformer jointly pretrained on 50 million pathology images and one billion clinical tokens. It aligns one million image-text pairs and supports 23 tasks, including classification, visual question answering, and outcome prediction, while enabling bidirectional image-text retrieval. MUSK exhibits strong cross-modal reasoning and partial generative capabilities. PathAsst [174] presents a task-oriented multimodal assistant tailored for pathology by integrating a specialized visual encoder (PathCLIP) with a Vicuna-based language model and curated expert-driven datasets. It supports diagnostic dialogue, report summarization, and decision reasoning through multimodal interaction, demonstrating generation-supportive capabilities via structured textual outputs conditioned on pathology images and task prompts.

*c) Generative Extensions:* These models primarily serve as robust visual encoders but can be extended to support downstream generative tasks when paired with decoders or prompt-based modules. GPFM [177], trained on 190 million pathology images from 86,000 WSIs across 34 tissue types, provides a universal visual backbone capable of powering downstream generation tasks such as report synthesis and visual question answering through fine-tuned generative heads. Similarly, PathoDuet [179] proposes a domain-adaptive self-supervised learning framework that incorporates two novel tasks: cross-scale positioning and cross-stain transferring, enabling the model to learn semantically aligned representations across magnifications and stain domains. While both GPFM and PathoDuet do not generate outputs natively, their architecture and pretrained embeddings are well-suited for generative extensions such as text-conditioned image manipulation or multimodal report generation.

Overall, multimodal generative models in computational pathology are transitioning from task-specific designs to unified frameworks that combine perception and generation. This evolution is marked by three trends: growing data scale and modality diversity, the use of transformer-based architectures with multimodal pretraining, and diverse generative strategies from explicit decoders

TABLE IV

OVERVIEW OF OTHER GENERATION METHODS IN COMPUTATIONAL PATHOLOGY, DETAILING INPUT TYPES, MODEL ARCHITECTURES, GENERATED OUTPUTS, AND APPLICATION TASKS.

Year	Name	Input	Model	Output	Application Task
2019	[24]	Patch	GAN	Representation	Classification, Segmentation
2023	PLIP [184]	Patch, Text	ViT	Representation	Classification, Retrieval
2024	HLSS [65]	Patch	LLM/VLM	Representation	Classification
2024	DiGress [185]	Cell graph	Diffusion	Cell graph	Classification, Biomarker prediction
2024	SynCellFactory [186]	Patch	Diffusion	Cell tracking	Segmentation, Classification, Detection
2024	KEP [187]	Patch, Text	ViT	Representation	Classification
2024	TANGLE [188]	WSI, Gene	ViT	Representation	Classification, Retrieval
2024	PLUTO [189]	Patch, WSI	ViT	Representation	Segmentation, Classification
2024	QAP [190]	Patch, WSI	LLM/VLM	Prompt	Classification, Report generation
2024	TQx [191]	Patch	LLM/VLM	Representation	Classification, Clustering
2024	[192]	Patch, Parameter	GAN	3D images	Segmentation
2024	[193]	Patch, Layout	Diffusion	Layout	Detection, Image generation
2024	TopoCellGen [194]	Cell layout	Diffusion	Layout	Segmentation, Classification
2024	PRDL [195]	Patch, WSI	Other	Representation	Classification
2024	AugDiff [196]	Patch, WSI	Diffusion	Representation	Classification
2024	DCDiff [197]	Patch, WSI	Diffusion	Representation	Classification
2025	DAMM-Diffusion [198]	Patch	Diffusion	Layout	Prognosis, Report generation
2025	THREADS [199]	WSI, Gene	LLM/VLM	Representation	Classification, Prognosis, Mutation prediction, Biomarker prediction
2025	Stem [200]	Patch	Diffusion	Representation	Biomarker Prediction
2025	MLLM4PUE [201]	Patch, Text	LLM/VLM	Representation	Retrieval, Classification
2025	LD-CVAE [84]	WSI, Gene	VAE	Gene	Prognosis
2025	MExD [68]	Feature	Diffusion	Representation	Retrieval, Classification

to representation-based designs. These developments reflect two paradigms: representation-centric models favor generalization, while generation-centric models enhance controllability. Progress toward integrated multimodal foundation models remains a cornerstone.

#### D. Other generation

Recent advances in generative modeling have expanded beyond traditional image and text synthesis to address a wider array of pathology-relevant data types. There are also many other generation tasks such as spatial layout generation, molecular/genomic data inference, textual and semantic output generation, latent feature generation, and synthetic image generation for segmentation or tracking.

**1) Spatial Layout Generation:** Generative models in this category aim to simulate biologically realistic spatial configurations of cellular or tissue structures, thereby enabling downstream tasks such as detection and classification under controlled topological assumptions. TopoCellGen [194] introduces a topology-aware diffusion framework that integrates persistent homology constraints into the generation process, enabling multi-class cell layouts that preserve inter- and intra-class spatial fidelity. [193] incorporates spatial priors from kernel density estimation and Gaussian mixture models to guide the diffusion process, conditioning generation on density-based cell layout maps. DiGress [185] leverages graph-based diffusion modeling to synthesize cell graphs that retain tertiary lymphoid structure (TLS) characteristics, contributing both to biomarker preservation and augmentation for TLS-related classification. DAMM-Diffusion [198] extends spatial layout modeling by predicting nanoparticle (NP) distributions within tumor microenvironments, using a multimodal diffusion framework that fuses structural components like vessels and nuclei through a divergence-aware predictor. Together, imposing topological and spatial constraints during cellular layout generation produces synthetically arranged microenvironments that faithfully preserve biological spatial relationships, enhancing both architectural realism and utility for downstream spatial analysis tasks.

**2) Molecular and Genomic Inference:** Many models aim to infer spatial or patient-level molecular profiles from histological images, effectively bridging the gap between morphology and genomics. Stem [200] employs a conditional diffusion model to generate spatial transcriptomics maps from H&E images, achieving biologically consistent predictions with high gene variation retention.

LD-CVAE [84] introduces a latent differentiation VAE to predict surrogate genomic embeddings from WSIs, enabling robust cancer survival prediction in scenarios lacking genomic data. TANGLE [188] aligns WSI and gene expression modalities via contrastive learning, providing a unified representation space for multimodal retrieval and few-shot learning. THREADS [199] represents the largest slide-level multimodal foundation model integrating H&E with genomic profiles, capturing underlying tissue molecular states and achieving superior performance in 54 oncology tasks. By enabling molecular-level inference directly from histology, these models hold promise for non-invasive, cost-efficient extensions to genomic diagnostics.

**3) Semantic Output Generation:** Semantic output generation focuses on generating semantically meaningful textual artifacts, such as prompts and embeddings, which facilitate interpretability, retrieval, and clinical decision support. QAP [190] introduces quantitative attribute-based prompting to translate spatial and morphological histological features into visual prompts for downstream model adaptation. MLLM4PUE [201] employs summarization-style prompts and multimodal large language models to generate universal embeddings, excelling in zero-shot classification and retrieval tasks. PLIP [184] trains on a large-scale internet-curated pathology dataset to generate joint image-text embeddings for bidirectional retrieval and interpretable classification, providing semantic alignment. TQx [191] generates text-based image embeddings by retrieving diagnostic keywords from a domain-specific vocabulary, thereby enabling explainable and clinically meaningful assessments without manual annotation. KEP [187] incorporates a structured pathology knowledge base into visual-language pretraining and projects expert-defined disease attributes into embedding space, significantly improving performance in zero-shot classification, retrieval, and tumor subtyping. These methods illustrate how generating semantically aligned outputs can support human-AI collaboration in clinical workflows.

**4) Latent Representation Generation:** Latent representation generation synthesizes intermediate representations or augments feature distributions in embedding space, enhancing robustness and efficiency. For example, [65] introduced a novel hierarchical language-tied self-supervision (HLSS) framework for histopathology image representation learning, expanding self-supervised learning objectives across patient, slide, and patch levels to generate improved latent representations, demonstrating superior performance on OpenSRH

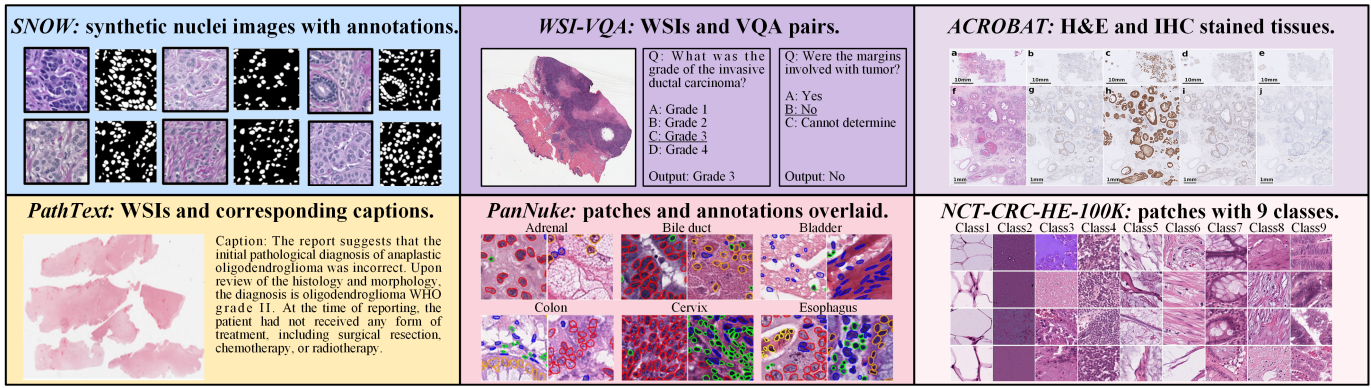


Fig. 9. Examples from representative pathology datasets showcasing variations in tissue type, staining, annotations, captions, and VQA pairs.

and TCGA datasets. Other approaches further refine or augment these representations; PRDL [195] augments multiple instance learning pipelines through prompt-guided latent space sampling, generating diverse WSI representations without costly image transformations. AugDiff [196] applies diffusion to generate semantically coherent feature-level augmentations, significantly improving generalization in gigapixel slide classification. MExD [68] combines a mixture-of-experts (MoE) aggregator with a diffusion-based generative classifier to synthesize class distributions, pioneering generative WSI classification. DCDiff [197] incorporates a dual-granularity cooperative diffusion architecture for feature generation across coarse and fine spatial resolutions, mimicking diagnostic reasoning at multiple scales. These works highlight a shift toward generative paradigms that operate in latent space, optimizing performance and scalability without relying solely on pixel-space synthesis.

5) **Cell Simulation:** Cell simulation focuses on generating synthetic microscopy data tailored for cell tracking and segmentation tasks, addressing the fundamental challenge of limited annotated data in biomedical imaging. SynCellFactory [186] introduces a specialized framework for time-lapse cell video synthesis that decouples motion dynamics from cellular appearance through complementary ControlNets, enabling the creation of photorealistic cell sequences with corresponding ground truth trajectories. Similarly, [192] presents a physics-informed GAN architecture that simultaneously generates coherent 3D cellular structures and their segmentation masks, incorporating biophysical constraints to ensure biological plausibility.

Overall, generative pathology has expanded from image synthesis to include spatial, molecular, semantic, and latent targets. Each paradigm serves distinct clinical goals: spatial and image generation support data augmentation, molecular inference enables precision medicine, semantic outputs improve interpretability, and latent modeling enhances computational efficiency. A systematic taxonomy offers a clear framework for understanding current research and guiding the development of future multimodal foundation models.

## IV. DATASET AND METRICS

### A. Datasets

To support the diverse generative tasks in computational pathology, we summarize commonly used datasets spanning a wide range of applications, including classification, segmentation, stain transformation, caption generation, and question answering, as detailed in Table V. These datasets span a broad range of organs, modalities (e.g., whole-slide images, image patches, and textual reports), and staining types (e.g., H&E and IHC), as illustrated in Fig. 9, offering a comprehensive foundation for the training and evaluation of generative models in computational pathology. Notably, with the recent

development of generative pathology, several synthetic benchmarks have emerged. These include both image-synthetic datasets, such as SNOW [102], which introduces a large-scale dataset of synthetic pathological images paired with semantic segmentation annotations for nuclei; and text-synthetic datasets, where generated textual reports or QA pairs are increasingly used to augment image-text training corpora. Examples include PathGen-1.6M [158], PathMMU [202], and WSI-VQA [163], which leverage large-scale language models to generate descriptive captions and question-answer pairs.

### B. Evaluation Metrics

To comprehensively assess the performance of generative models in digital pathology, a diverse set of evaluation metrics is employed, each capturing different aspects of image quality, biological fidelity, and task relevance. These metrics can be broadly categorized into six groups: *perceptual quality*, *distribution divergence*, *structural fidelity*, *language similarity*, *pixel-level error*, and *expert judgment*. Perceptual quality metrics, such as FID and LPIPS, measure the visual realism and feature-level similarity between generated and real images. Distribution-based metrics, including KL divergence and Wasserstein Distance, evaluate the alignment between feature or latent distributions. Structural fidelity metrics focus on preserving biologically relevant spatial patterns, such as cellular morphology and tissue organization, using metrics like IoU and cell shape similarity. Language similarity metrics (e.g., BLEU, METEOR) are employed primarily in text-to-image or report-conditioned generation to evaluate semantic alignment. Pixel-level error metrics like MSE and PSNR quantify reconstruction fidelity at the pixel scale. Lastly, expert judgment metrics capture subjective evaluations from pathologists, offering practical insight into the clinical acceptability of generated outputs. Table VI summarizes the representative metrics in each category, along with their definitions and mathematical formulations.

## V. DISCUSSION

### A. Open Challenges

Despite rapid progress, generative pathology continues to face core challenges such as data scarcity, computational inefficiency, inadequate evaluation frameworks, and unresolved ethical concerns, all of which hinder clinical translation and scalable deployment.

**WSI Generation.** The synthesis of realistic whole-slide images (WSIs) remains a significant challenge due to their gigapixel-scale resolution and the scarcity of comprehensively annotated training data. Current patch-based approaches effectively capture local histological patterns but frequently fail to preserve global spatial coherence and tissue-wide architectural integrity. This limitation substantially

TABLE V

COMMONLY USED DATASETS IN GENERATIVE AND COMPUTATIONAL PATHOLOGY. THIS TABLE SUMMARIZES WIDELY USED DATASETS ACROSS TASKS SUCH AS IMAGE SYNTHESIS, STAIN TRANSFER, SEGMENTATION, CLASSIFICATION, CAPTIONING, AND QUESTION ANSWERING, ETC.

Dataset	Usage	Organ	Modality	Type	Size	Link	Authenticity
ACROBAT [203]	Strain transfer	Breast	WSI	H&E, IHC	4,212 WSIs	<a href="https://acrobot.grand-challenge.org/">https://acrobot.grand-challenge.org/</a>	Real
BCI [204]	Strain transfer	Breast	WSI	H&E, IHC	9746 images	<a href="https://bci.grand-challenge.org/">https://bci.grand-challenge.org/</a>	Real
EMPaCT [205]	Strain transfer	Prostate	Patch	H&E, IHC	210 pairs	<a href="https://zenodo.org/records/10066853">https://zenodo.org/records/10066853</a>	Real
ARCH [206]	Segmentation, Detection, Retrieval	Multiple	Patch	/	15,164 images	<a href="https://warwick.ac.uk/fac/cross_fac/tia/data/arch">https://warwick.ac.uk/fac/cross_fac/tia/data/arch</a>	Real
Camelyon16 [207]	Segmentation, Detection	Breast	WSI	H&E	400 WSIs	<a href="https://camelyon16.grand-challenge.org/Home/">https://camelyon16.grand-challenge.org/Home/</a>	Real
DigestPath [208]	Segmentation, Detection	Multiple	Patch	H&E	1559 images	<a href="https://digestpath2019.grand-challenge.org/Home/">https://digestpath2019.grand-challenge.org/Home/</a>	Real
CoNIC [209]	Segmentation, Classification	Colon	Patch	H&E	4981 images	<a href="https://conic-challenge.grand-challenge.org/">https://conic-challenge.grand-challenge.org/</a>	Real
CoNSeP [210]	Segmentation, Classification	Colon	Patch	H&E	41 images	<a href="https://opendatalab.com/OpenDataLab/CoNSeP">https://opendatalab.com/OpenDataLab/CoNSeP</a>	Real
PanNuke [211]	Segmentation, Classification	Multiple	Patch	H&E	7,901 images	<a href="https://huggingface.co/datasets/RationAI/PanNuke">https://huggingface.co/datasets/RationAI/PanNuke</a>	Real
TCGA READ	Segmentation, Classification	Colon	WSI	H&E	172 Cases, 9,871 Files, 1,194 Annotations	<a href="https://portal.gdc.cancer.gov/projects/TCGA-READ">https://portal.gdc.cancer.gov/projects/TCGA-READ</a>	Real
TCGA-BRCA	Segmentation, Classification	Breast	WSI	H&E	1,098 Cases, 68,962 Files, 6,934 Annotations	<a href="https://portal.gdc.cancer.gov/projects/TCGA-BRCA">https://portal.gdc.cancer.gov/projects/TCGA-BRCA</a>	Real
BCSS [212]	Segmentation	Breast	WSI	H&E	151 WSIs	<a href="https://github.com/PathologyDataScience/BCSS">https://github.com/PathologyDataScience/BCSS</a>	Real
GlaS [213]	Segmentation	Multiple	Patch	H&E	165 images	<a href="https://www.kaggle.com/datasets/sani84/glasticcai2015-gland-segmentation">https://www.kaggle.com/datasets/sani84/glasticcai2015-gland-segmentation</a>	Real
Lizard [214]	Segmentation	Colon	Patch	H&E	495,179 labelled nuclei	<a href="https://www.kaggle.com/datasets/aadimator/lizard-dataset">https://www.kaggle.com/datasets/aadimator/lizard-dataset</a>	Real
MoNuSeg [215]	Segmentation	Multiple	Patch	H&E	29,000 nuclei boundary from 44 WSIs	<a href="https://monuseg.grand-challenge.org/">https://monuseg.grand-challenge.org/</a>	Real
SegPath [216]	Segmentation	Multiple	WSI	H&E	158,687 images	<a href="https://dakomura.github.io/SegPath/">https://dakomura.github.io/SegPath/</a>	Real
WSSS4LUAD [217]	Segmentation	Lung	Patch, WSI	H&E	10,211 images	<a href="https://wsss4luad.grand-challenge.org/WSSS4LUAD/">https://wsss4luad.grand-challenge.org/WSSS4LUAD/</a>	Real
SNOW [218]	Segmentation	Breast	Patch	H&E	20000 images	<a href="https://zenodo.org/records/6633721#.YuE33OzMJHE">https://zenodo.org/records/6633721#.YuE33OzMJHE</a>	Image synthetic
QUILT-1M [219]	Retrieval, Caption generation, QA	Multiple	Patch	/	1,000,000 image-text pairs	<a href="https://zenodo.org/records/8239942">https://zenodo.org/records/8239942</a>	Real
PathText [157]	Report generation	Multiple	Patch, Text	/	9009 WSI-text pairs	<a href="https://github.com/cpystan/Wsi-Caption">https://github.com/cpystan/Wsi-Caption</a>	Text synthetic
PathMMU [202]	QA	Multiple	Patch, Text	/	24,067 images of 33,428 multi-choice questions	<a href="https://huggingface.co/datasets/jamesyxp/PathMMU">https://huggingface.co/datasets/jamesyxp/PathMMU</a>	Text synthetic
PathVQA [170]	QA	Multiple	Patch, Text	/	5,004 images, 32,795 QA pairs	<a href="https://huggingface.co/datasets/flaviagiannarino/path-vqa">https://huggingface.co/datasets/flaviagiannarino/path-vqa</a>	Text synthetic
PMC-VQA [220]	QA	Multiple	Patch, Text	Mutiple	227k VQA pairs of 149k images	<a href="https://huggingface.co/datasets/RadGenome/PMC-VQA">https://huggingface.co/datasets/RadGenome/PMC-VQA</a>	Text synthetic
QUILT-VQA [154]	QA	Multiple	Patch, Text	/	985 images, 1283 QA pairs	<a href="https://huggingface.co/datasets/wisdomik/Quilt_VQA">https://huggingface.co/datasets/wisdomik/Quilt_VQA</a>	Text synthetic
WSI-VQA [163]	QA	Breast	WSI, Text	H&E	977 WSIs, 8,672 QA pairs	<a href="https://github.com/cpystan/WSI-VQA">https://github.com/cpystan/WSI-VQA</a>	Text synthetic
TUPAC16 [221]	Detection, Classification	Breast	WSI	H&E	573 cases	<a href="https://tupac.grand-challenge.org/">https://tupac.grand-challenge.org/</a>	Real
PAIP2021	Detection	Multiple	WSI	H&E	240 WSIs	<a href="https://paip2021.grand-challenge.org">https://paip2021.grand-challenge.org</a>	Real
HEST-1k [222]	Biomarker exploration	Multiple	WSI, transcriptomics, metadata	H&E	1,229 cases	<a href="https://huggingface.co/datasets/MahmoodLab/HEst">https://huggingface.co/datasets/MahmoodLab/HEst</a>	Real
OpenPath [184]	Classification, Retrieval	Multiple	Patch, Text	/	208,414 images with descriptions	<a href="https://huggingface.co/spaces/vinid/webclip">https://huggingface.co/spaces/vinid/webclip</a>	Real
BRACS [223]	Classification, Detection	Breast	WSI	H&E	547 WSIs	<a href="https://www.bracs.icar.cnr.it/">https://www.bracs.icar.cnr.it/</a>	Real
EndoNuke [224]	Classification, Detection	Uterus	Patch	IHC	1780 images	<a href="https://endonuke.ispras.ru/">https://endonuke.ispras.ru/</a>	Real
BACH [225]	Classification	Breast	Patch, WSI	H&E	400+ images	<a href="https://zenodo.org/records/3632035">https://zenodo.org/records/3632035</a>	Real
BCNB [226]	Classification	Breast	WSI	H&E	1058 WSIs	<a href="https://bcnb.grand-challenge.org/">https://bcnb.grand-challenge.org/</a>	Real
BreakHis [227]	Classification	Breast	Patch	H&E	9,709 images	<a href="https://web.inf.ufpr.br/vri/databases/breast-cancer-histopathological-database-b">https://web.inf.ufpr.br/vri/databases/breast-cancer-histopathological-database-b</a>	Real
Camelyon17 [228]	Classification	Breast	WSI	H&E	1399 WSIs	<a href="https://camelyon17.grand-challenge.org/Home/">https://camelyon17.grand-challenge.org/Home/</a>	Real
CRC-VAL-HE-7K [229]	Classification	Colon	Patch	H&E	7,180 images	<a href="https://zenodo.org/records/1214456">https://zenodo.org/records/1214456</a>	Real
H&ER2 [230]	Classification	Breast	WSI	H&E	273 WSIs	<a href="https://www.cancerimagingarchive.net/collection/HER2-tumor-rois/">https://www.cancerimagingarchive.net/collection/HER2-tumor-rois/</a>	Real
ICIAR-BACH-2018 [231]	Classification	Breast	Patch	H&E	400 images	<a href="https://iciar2018-challenge.grand-challenge.org/Dataset/">https://iciar2018-challenge.grand-challenge.org/Dataset/</a>	Real
LC25000 [232]	Classification	Multiple	Patch	H&E	25,000 images	<a href="https://www.kaggle.com/datasets/andrewmvd/lung-and-colon-cancer-histopatho-data">https://www.kaggle.com/datasets/andrewmvd/lung-and-colon-cancer-histopatho-data</a>	Real
MHIST [233]	Classification	Colon	Patch	H&E	3,152 images	<a href="https://bmirids.github.io/MHIST/">https://bmirids.github.io/MHIST/</a>	Real
NCT-CRC-HE-100K [229]	Classification	Colon	Patch	H&E	100000 images	<a href="https://zenodo.org/records/1214456">https://zenodo.org/records/1214456</a>	Real
PANDA [234]	Classification	Prostate	WSI	H&E	about 11,000 WSIs	<a href="https://www.kaggle.com/c/prostate-cancer-grade-assessment/overview">https://www.kaggle.com/c/prostate-cancer-grade-assessment/overview</a>	Real
PatchCamelyon [235]	Classification	Multiple	Patch	H&E	327,680 images	<a href="https://github.com/basveeling/pcam">https://github.com/basveeling/pcam</a>	Real
SICAPv2 [236]	Classification	Prostate	WSI	H&E	155 biopsies	<a href="https://data.mendeley.com/datasets/9xxm58dvs3/1">https://data.mendeley.com/datasets/9xxm58dvs3/1</a>	Real
TCGA-BLCA	Classification	Bladder	WSI	H&E	412 Cases, 29,345 Files, 2,283 Annotations	<a href="https://portal.gdc.cancer.gov/projects/TCGA-BLCA">https://portal.gdc.cancer.gov/projects/TCGA-BLCA</a>	Real
TCGA-COAD	Classification	Colon	WSI	H&E	461 Cases, 28,133 Files, 3,547 Annotations	<a href="https://portal.gdc.cancer.gov/projects/TCGA-COAD">https://portal.gdc.cancer.gov/projects/TCGA-COAD</a>	Real
TCGA-LUAD	Classification	Lung	WSI	H&E	585 Cases, 35,035 Files, 3,934 Annotations	<a href="https://portal.gdc.cancer.gov/projects/tcga-luad">https://portal.gdc.cancer.gov/projects/tcga-luad</a>	Real
PathGen-1.6M [158]	Caption generation	Multiple	Patch, Text	Mutiple	1,600,000 image-text pairs	<a href="https://huggingface.co/datasets/jamesyxp/PathGen">https://huggingface.co/datasets/jamesyxp/PathGen</a>	Text synthetic
PatchGastricADC22 [237]	Caption generation	Stomach	Patch, Text	H&E	262k images	<a href="https://zenodo.org/records/6021442">https://zenodo.org/records/6021442</a>	Real
PathCap [174]	Caption generation	Multiple	Patch, Text	/	207K image-caption pairs	<a href="https://huggingface.co/datasets/jamesyxp/PathCap">https://huggingface.co/datasets/jamesyxp/PathCap</a>	Real

impairs their utility for applications requiring long-range contextual information, such as tumor staging and morphological heterogeneity assessment. While hierarchical generation frameworks and multiscale attention mechanisms offer promising directions by modeling cross-scale dependencies, they impose prohibitive computational demands that render them largely impractical on standard hardware. Developing memory-efficient, resolution-aware architectures represents a critical research priority to enable the modeling of complex spatial

relationships in histopathological data and advance WSI synthesis toward clinical viability.

**Generation Efficiency.** Generative models in computational pathology face three critical efficiency challenges that hinder their clinical integration. First, limited annotated data availability, especially for rare histological variants, restricts the learning of comprehensive generative distributions, compromising synthesis quality in low-resource contexts. Second, inherent data imbalances across

TABLE VI

SUMMARY OF COMMONLY USED METRICS FOR EVALUATING GENERATION WITH STANDARD DEFINITIONS AND CORE FORMULAS.

Category	Metric (Abbr.)	Definition	Formula
Perceptual Quality	Fréchet Inception Distance (FID) [238]	Measures distribution distance between generated images (P) and real images (Q) in inception feature space.	$FID = \ \mu_P - \mu_Q\ ^2 + \text{Tr}(\sum_P + \sum_Q - 2(\sum_P \sum_Q)^{\frac{1}{2}})$
Perceptual Quality	Patch-based FID (pFID) [239]	Local FID on patches for structure fidelity.	$pFID = \frac{1}{N} \sum_{i=1}^N FID(x_i^{\text{patch}}, y_i^{\text{patch}})$
Perceptual Quality	Inception Score (IS) [240]	Evaluates image diversity and clarity using a pre-trained Inception network.	$IS = \exp(\mathbb{E}_{x \sim P} [D_{KL}(p(y x)  p(y))])$
Perceptual Quality	Learned Perceptual Image Patch Similarity (LPIPS) [241]	Computes perceptual similarity using deep network features.	$LPIPS(x, \hat{x}) = \sum_l \ w_l \odot (\phi_l^x - \phi_l^{\hat{x}})\ _2^2$
Perceptual Quality	Structural Similarity Index (SSIM) [242]	Measures structural similarity between images based on luminance, contrast, and structure.	$SSIM(x, y) = \frac{(2\mu_x\mu_y + C_1)(2\sigma_{xy} + C_2)}{(\mu_x^2 + \mu_y^2 + C_1)(\sigma_x^2 + \sigma_y^2 + C_2)}$
Perceptual Quality	Feature Similarity Index (FSIM) [243]	Uses phase congruency (PC) and gradient magnitude (GM) to assess visual quality.	$FSIM = \frac{\sum_{x \in \Omega} S_L(x) \cdot PC_m(x)}{\sum_{x \in \Omega} PC_m(x)}$
Perceptual Quality	Gradient Magnitude Similarity Deviation (GMSD) [244]	Evaluates edge and gradient consistency.	$GMSD = \sqrt{\frac{1}{N} \sum_{i=1}^N (GMS_i - \mu_{GMS})^2}$
Perceptual Quality	Consensus-based Image Description Evaluation (CIDEr) [245]	Measures semantic and perceptual consistency between image and text.	$CIDEr = \frac{1}{m} \sum_{j=1}^m \frac{g^n(x_i) \cdot g^n(y_{ij})}{\ g^n(x_i)\  \ g^n(y_{ij})\ }$
Perceptual Quality	Luminance Contrast (LC) [246]	Evaluates contrast consistency in luminance.	$LC = \frac{x_{\max} - x_{\min}}{x_{\max} + x_{\min}}$
Pixel-level Error	Mean Squared Error (MSE) [247]	Average of squared differences between pixels.	$MSE = \frac{1}{N} \sum_{i=1}^N (x_i - \hat{x}_i)^2$
Pixel-level Error	Mean Absolute Error (MAE) [248]	Mean of absolute pixel difference.	$MAE = \frac{1}{N} \sum_{i=1}^N  x_i - \hat{x}_i $
Pixel-level Error	Normalized Root Mean Square Error (NRMSE) [249]	Square root of MSE divided by value range or mean of reference.	$NRMSE = \frac{\sqrt{MSE}}{x_{\max} - x_{\min}}$
Pixel-level Error	Peak Signal-to-Noise Ratio (PSNR) [250]	High PSNR implies better image reconstruction, based on pixel-wise fidelity.	$PSNR = 10 \cdot \log_{10} \left( \frac{MAX^2}{MSE} \right)$
Distribution Divergence	Kolmogorov–Smirnov Test (KS) [251]	Non-parametric test for comparing sample distributions.	$KS = \max  F_1(x) - F_2(\hat{x}) $
Distribution Divergence	Wasserstein Distance (WD) [252]	Earth mover's distance, measures the minimal cost of transforming one distribution to another.	$WD(P, Q) = \inf_{\gamma \in \Pi(P, Q)} \mathbb{E}_{(x, y) \sim \gamma} \ x - y\ $
Distribution Divergence	Jensen–Shannon Divergence (JSD) [253]	Symmetric divergence between two probability distributions.	$JSD(P  Q) = \frac{1}{2} \left[ D_{KL} \left( P    \frac{P+Q}{2} \right) + D_{KL} \left( Q    \frac{P+Q}{2} \right) \right]$
Distribution Divergence	Kullback–Leibler Divergence (KL) [254]	Measures information loss between two distributions (asymmetric).	$D_{KL}(P  Q) = \sum_i P(x_i) \log \frac{P(x_i)}{Q(x_i)}$
Distribution Divergence	Maximum Mean Discrepancy (MMD) [255]	Kernel-based test for distributional similarity between samples.	$MMD = \sup E_P[f(x)] - E_Q[f(y)]$
Distribution Divergence	Kernel Inception Distance (KID) [256]	Similar to FID but more stable on small datasets.	$KID = \sup_{f \in H} E_P f(x) - E_Q f(y)$
Structural Fidelity	Intersection over Union (IoU) [257]	Measures overlap between predicted and ground truth masks.	$IoU = \frac{ x \cap y }{ x \cup y }$
Structural Fidelity	Pearson Correlation Coefficient (PC) [258]	Measures linear correlation between two variables or images.	$PC = \frac{\sum_i (x_i - \bar{x})(y_i - \bar{y})}{\sqrt{\sum_i (x_i - \bar{x})^2 \sum_i (y_i - \bar{y})^2}}$
Structural Fidelity	Precision [259]	Fraction of predicted positives that are correct.	$Precision = \frac{TP}{TP + FP}$
Structural Fidelity	Recall [260]	Fraction of actual positives correctly identified.	$Recall = \frac{TP}{TP + FN}$
Language Similarity	BiLingual Evaluation Understudy (BLEU-1,2,3,4) [261]	Calculates n-gram precision between generated and reference texts.	$BLEU = BP \cdot \exp \left( \sum_{n=1}^N w_n \log p_n \right)$
Language Similarity	Recall-Oriented Understudy for Gisting Evaluation (ROUGE-L) [262]	Measures similarity based on longest common subsequence (LCS), emphasizing recall.	$ROUGE-L = \frac{(1 + \beta^2) \cdot LCS}{R + \beta^2 \cdot C}$
Language Similarity	Metric for Evaluation of Translation with Explicit Ordering (METEOR) [263]	Measures text similarity with unigram matches and word order penalty.	$METEOR = F_{mean} \cdot (1 - Penalty)$
Expert Judgment	Pathologist Preference [264]	Subjective scoring or ranking by pathologists.	$Preference\ Score = \frac{1}{N} \sum_{i=1}^N rating_i$

anatomical sites, disease types, and staining protocols introduce representational biases favoring common phenotypes while inadequately capturing long-tail distributions, thereby reducing the effectiveness of synthetic data for holistic augmentation. Third, contemporary architectures such as diffusion models impose prohibitive computational demands during inference, with their iterative denoising processes making real-time clinical deployment impractical. Although recent architectural innovations like multiscale modeling and semantic conditioning have improved output fidelity, they simultaneously increase computational complexity and memory requirements. Addressing these efficiency constraints through optimized sampling algorithms, few-shot adaptation techniques, and hardware-aware implementations

remains essential for enabling the practical deployment of generative models in clinical pathology workflows.

**Evaluation Limitation.** The absence of standardized and domain-specific evaluation protocols remains a critical barrier to the progress and clinical applicability of generative models in computational pathology. Conventional metrics such as FID, SSIM, and PSNR, originally developed for natural image assessment, primarily measure low-level visual similarity and are inadequate for capturing diagnostic features essential in histopathology, including cellular morphology, glandular architecture, and spatial tissue organization. This misalignment risks the generation of visually plausible yet clinically irrelevant or misleading outputs. Although efforts have been made to introduce

domain-aware evaluation criteria, these remain fragmented and lack validation across diverse datasets and pathological conditions. Moreover, unlike the natural image domain, computational pathology lacks standardized benchmark datasets and evaluation protocols, hindering fair and reproducible comparisons. Establishing robust, pathology-specific benchmarks and multidimensional evaluation frameworks is crucial for systematic assessment and progress.

**Computational Cost.** Generative frameworks, particularly diffusion-based models, present substantial computational demands that limit their scalability and clinical integration. These models require hundreds of iterative denoising steps, resulting in high memory consumption and prolonged inference times. The challenge is exacerbated in high-resolution histopathological images, where computational complexity scales with image dimensions, making gigapixel whole-slide image generation impractical on standard hardware. Furthermore, lengthy training cycles raise development costs and hinder iterative experimentation.

**Ethical, Legal, and Security Considerations.** The integration of synthetic data in computational pathology introduces multifaceted challenges across ethical, legal, and security domains [265] that require systematic examination before clinical implementation. Ethically, synthetically generated histopathological images may present visual verisimilitude while harboring biological inconsistencies, potentially compromising diagnostic accuracy by misleading both algorithms and human experts—a critical concern in high-stakes clinical environments where interpretability underpins trust. From a legal perspective, the regulatory framework governing synthetic medical data remains underdeveloped, with crucial issues including patient consent boundaries, intellectual property rights, and liability for diagnostic errors stemming from synthetic data utilization inadequately addressed in current healthcare governance structures. Security vulnerabilities emerge when models trained on synthetic distributions exhibit reduced robustness against adversarial manipulations, particularly when these distributions fail to capture the complex heterogeneity and edge cases present in clinical specimens.

## B. Future Opportunities

The advancement of generative models in computational pathology demands deeper integration of data modalities, model capabilities, and clinical needs. Future works prioritize unified architectures, multimodal generation, robust evaluation, and clinical interpretability.

**Generative Foundation Model.** A key future direction involves the development of general-purpose generative foundation models specifically designed for computational pathology. Current foundation models [266] that are limited to narrow tasks or focus on representation learning, future architectures should aim to integrate multiple generative functionalities within a single unified framework. These include whole-slide image synthesis, mask-conditioned augmentation, semantic report generation, and molecular prediction. By constructing shared latent spaces and employing scalable pretraining strategies, such models can enable multi-objective learning across image, textual, and molecular modalities. This unified approach holds promise for addressing persistent challenges such as data scarcity, class imbalance, and fragmented task pipelines. Furthermore, it may enhance few-shot generalization and cross-domain transferability with minimal supervision, thereby supporting the development of efficient, adaptable, and clinically applicable generative systems.

**Multimodal Generative Pathology.** Future advances in generative modeling for computational pathology are expected to move toward fully multimodal architectures that integrate histological imaging, genomic information, molecular markers, and clinical metadata. These models should support cross-modal generation tasks, including

image-to-text, text-to-image, and gene-to-image synthesis, thereby enabling comprehensive and biologically grounded disease representation. Ensuring semantic consistency across modalities will require the development of unified latent spaces and alignment strategies that preserve clinically meaningful correlations between modalities. Additionally, incorporating temporal information into generative models remains an open research area. Leveraging sequential histological data together with longitudinal clinical records may enable the modeling of disease evolution over time, offering new opportunities for predictive pathology and personalized treatment planning.

**Unified Evaluation.** Establishing a comprehensive evaluation framework for pathology generation models constitutes a pivotal bridge between technical development and clinical implementation. Our proposed tripartite assessment structure, encompassing visual fidelity, structural integrity, and semantic relevance, mirrors the fundamental cognitive progression in pathological analysis from morphological perception to diagnostic interpretation. The framework integrates expert-blinded evaluation protocols with quantitative downstream task performance metrics and cross-domain generalization assessments, enabling robust validation aligned with clinical workflows. This methodological integration facilitates precise discrimination between model capabilities while ensuring reliability and clinical adaptability in translational contexts, ultimately advancing computational pathology toward clinically meaningful implementation.

**Explainability and Reliability.** Despite the promising capabilities of generative models in pathology, limited interpretability and reliability remain critical barriers to clinical adoption. Generated outputs, particularly those used for diagnosis, prediction, or reporting, must be transparent and justifiable to ensure trust and accountability. To address this challenge, future work should incorporate multi-level interpretability strategies such as visual attribution maps, uncertainty quantification, and semantic reasoning modules that align with pathological criteria. In addition, expert-in-the-loop evaluation involving certified pathologists is essential to validate model decisions, identify potential failure modes, and refine generation quality. Beyond technical transparency, comprehensive fairness audits are necessary to detect demographic or disease-specific biases and to ensure robust performance across diverse clinical scenarios. Establishing these mechanisms is fundamental to transitioning generative pathology models from experimental systems to clinically trusted tools.

## VI. CONCLUSION

Generative modeling has rapidly gained traction in computational pathology, marking a pivotal shift in how synthetic data, multimodal integration, and cross-scale learning are approached. This survey systematically reviewed the growing landscape of generative modeling in computational pathology by organizing recent advances into four major categories: image generation, text generation, multimodal generation, and other specialized generative tasks. The growing body of literature highlights not only methodological innovation, ranging from GANs and diffusion models to LLM/VLM-powered architectures, but also a broader redefinition of what generative modeling can accomplish beyond image synthesis. This survey offers a structured overview of generative modeling in computational pathology, categorizing methods by task objectives and data modalities. As the field progresses, unified generative foundation models that integrate clinical, molecular, and textual data are expected to drive scalable and trustworthy solutions. We hope this review serves as a reference point for future developments in this rapidly advancing domain.

## REFERENCES

- [1] B. van Breugel *et al.*, “Synthetic data in biomedicine via generative artificial intelligence,” *Nature Reviews Bioengineering*, vol. 2, no. 12, pp. 991–1004, 2024.
- [2] A. Zhang *et al.*, “Shifting machine learning for healthcare from development to deployment and from models to data,” *Nature biomedical engineering*, vol. 6, no. 12, pp. 1330–1345, 2022.
- [3] A. Kazerouni *et al.*, “Diffusion models in medical imaging: A comprehensive survey,” *Medical image analysis*, vol. 88, p. 102846, 2023.
- [4] A. H. Song *et al.*, “Artificial intelligence for digital and computational pathology,” *Nature Reviews Bioengineering*, vol. 1, no. 12, pp. 930–949, 2023.
- [5] F.-A. Croitoru *et al.*, “Diffusion models in vision: A survey,” *IEEE Transactions on Pattern Analysis and Machine Intelligence*, vol. 45, no. 9, pp. 10850–10869, 2023.
- [6] C. He *et al.*, “Diffusion models in low-level vision: A survey,” *IEEE Transactions on Pattern Analysis and Machine Intelligence*, 2025.
- [7] Z. Guo *et al.*, “Diffusion models in bioinformatics and computational biology,” *Nature reviews bioengineering*, vol. 2, no. 2, pp. 136–154, 2024.
- [8] I. Goodfellow *et al.*, “Generative adversarial networks,” *Commun. ACM*, vol. 63, no. 11, p. 139–144, Oct. 2020.
- [9] Z. Ju *et al.*, “HAGAN: hybrid augmented generative adversarial network for medical image synthesis,” *CoRR*, vol. abs/2405.04902, 2024. [Online]. Available: <https://doi.org/10.48550/arXiv.2405.04902>
- [10] H. Cho *et al.*, “Neural stain-style transfer learning using gan for histopathological images,” 2017. [Online]. Available: <https://arxiv.org/abs/1710.08543>
- [11] Y. Shen *et al.*, “A federated learning system for histopathology image analysis with an orchestral stain-normalization gan,” *IEEE Transactions on Medical Imaging*, vol. 42, no. 7, pp. 1969–1981, 2023.
- [12] N. Bouteldja *et al.*, “Tackling stain variability using cyclegan-based stain augmentation,” *Journal of Pathology Informatics*, vol. 13, p. 100140, 2022.
- [13] A. Radford, L. Metz, and S. Chintala, “Unsupervised representation learning with deep convolutional generative adversarial networks,” 2016. [Online]. Available: <https://arxiv.org/abs/1511.06434>
- [14] M. Arjovsky, S. Chintala, and L. Bottou, “Wasserstein gan,” 2017. [Online]. Available: <https://arxiv.org/abs/1701.07875>
- [15] T. Karras *et al.*, “Progressive growing of gans for improved quality, stability, and variation,” 2018. [Online]. Available: <https://arxiv.org/abs/1710.10196>
- [16] F. G. Zanjani *et al.*, “Stain normalization of histopathology images using generative adversarial networks,” in *2018 IEEE 15th International Symposium on Biomedical Imaging (ISBI 2018)*, 2018, pp. 573–577.
- [17] M. Runz *et al.*, “Normalization of he-stained histological images using cycle consistent generative adversarial networks,” *Diagnostic Pathology*, vol. 16, no. 1, p. 71, 08 2021. [Online]. Available: <https://doi.org/10.1186/s13000-021-01126-y>
- [18] J. Breen *et al.*, “Generative adversarial networks for stain normalisation in histopathology,” in *Applications of Generative AI*. Springer, 2024, pp. 227–247.
- [19] Z. Du *et al.*, “Deeply supervised two stage generative adversarial network for stain normalization,” *Scientific Reports*, vol. 15, no. 1, p. 7068, 02 2025.
- [20] M. Kawai *et al.*, “Virtual multi-staining in a single-section view for renal pathology using generative adversarial networks,” *Computers in biology and medicine*, vol. 182, pp. 109149–109149, 2024.
- [21] S. Liu *et al.*, “Unpaired stain transfer using pathology-consistent constrained generative adversarial networks,” *IEEE Transactions on Medical Imaging*, vol. 40, no. 8, pp. 1977–1989, 2021.
- [22] M. Liang *et al.*, “Multi-scale self-attention generative adversarial network for pathology image restoration,” *The Visual Computer*, vol. 39, no. 9, pp. 4305–4321, 09 2023. [Online]. Available: <https://doi.org/10.1007/s00371-022-02592-1>
- [23] R. Rong *et al.*, “Enhanced pathology image quality with restore-generative adversarial network,” *The American Journal of Pathology*, vol. 193, no. 4, pp. 404–416, 2023.
- [24] B. Hu *et al.*, “Unsupervised learning for cell-level visual representation in histopathology images with generative adversarial networks,” *IEEE Journal of Biomedical and Health Informatics*, vol. 23, no. 3, pp. 1316–1328, 2019.
- [25] M. Mirza and S. Osindero, “Conditional generative adversarial nets,” 2014. [Online]. Available: <https://arxiv.org/abs/1411.1784>
- [26] P. Isola *et al.*, “Image-to-image translation with conditional adversarial networks,” in *Proceedings of the IEEE conference on computer vision and pattern recognition*, 2017, pp. 1125–1134.
- [27] T. Karras, S. Laine, and T. Aila, “A style-based generator architecture for generative adversarial networks,” 2019. [Online]. Available: <https://arxiv.org/abs/1812.04948>
- [28] Y. Lin *et al.*, “Insmix: Towards realistic generative data augmentation for nuclei instance segmentation,” 2022. [Online]. Available: <https://arxiv.org/abs/2206.15134>
- [29] C. D. Bahadir *et al.*, “Characterizing the features of mitotic figures using a conditional diffusion probabilistic model,” in *International Conference on Medical Image Computing and Computer-Assisted Intervention*. Springer, 2023, pp. 121–131.
- [30] A. Golfe *et al.*, “Progleason-gan: Conditional progressive growing gan for prostatic cancer gleason grade patch synthesis,” *Computer Methods and Programs in Biomedicine*, vol. 240, p. 107695, 2023.
- [31] S. Min, H.-J. Oh, and W.-K. Jeong, “Co-synthesis of histopathology nuclei image-label pairs using a context-conditioned joint diffusion model,” in *Computer Vision – ECCV 2024*, A. Leonardis *et al.*, Eds. Cham: Springer Nature Switzerland, 2025, pp. 146–162.
- [32] M. Li *et al.*, “Unified framework for histopathology image augmentation and classification via generative models,” in *2024 International Conference on Digital Image Computing: Techniques and Applications (DICTA)*. IEEE, 2024, pp. 462–469.
- [33] J. Ho, A. Jain, and P. Abbeel, “Denoising diffusion probabilistic models,” in *Advances in Neural Information Processing Systems*, H. Larochelle *et al.*, Eds., vol. 33. Curran Associates, Inc., 2020, pp. 6840–6851.
- [34] P. Dhariwal and A. Nichol, “Diffusion models beat gans on image synthesis,” in *Proceedings of the 35th International Conference on Neural Information Processing Systems*, ser. NIPS ’21. Red Hook, NY, USA: Curran Associates Inc., 2021.
- [35] L. Yang *et al.*, “Diffusion models: A comprehensive survey of methods and applications,” *ACM Comput. Surv.*, vol. 56, no. 4, Nov. 2023. [Online]. Available: <https://doi.org/10.1145/3626235>
- [36] Y. Song and S. Ermon, *Generative modeling by estimating gradients of the data distribution*. Red Hook, NY, USA: Curran Associates Inc., 2019.
- [37] S. Lim *et al.*, “Score-based generative modeling through stochastic evolution equations in hilbert spaces,” in *Proceedings of the 37th International Conference on Neural Information Processing Systems*, ser. NIPS ’23. Red Hook, NY, USA: Curran Associates Inc., 2023.
- [38] A. Shrivastava and P. T. Fletcher, “NASDM: nuclei-aware semantic histopathology image generation using diffusion models,” *CoRR*, vol. abs/2303.11477, 2023. [Online]. Available: <https://doi.org/10.48550/arXiv.2303.11477>
- [39] M. Sun *et al.*, “Enhancing gland segmentation in colon histology images using an instance-aware diffusion model,” *Computers in Biology and Medicine*, vol. 166, p. 107527, 2023.
- [40] H.-J. Oh and W.-K. Jeong, “Diffmix: Diffusion model-based data synthesis for nuclei segmentation and classification in imbalanced pathology image datasets,” in *International Conference on Medical Image Computing and Computer-Assisted Intervention*. Springer, 2023, pp. 337–345.
- [41] X. Yu *et al.*, “Diffusion-based data augmentation for nuclei image segmentation,” in *Medical Image Computing and Computer Assisted Intervention – MICCAI 2023*, H. Greenspan *et al.*, Eds. Cham: Springer Nature Switzerland, 2023, pp. 592–602.
- [42] M. Aversa *et al.*, “Diffinfinite: Large mask-image synthesis via parallel random patch diffusion in histopathology,” in *Advances in Neural Information Processing Systems*, A. Oh *et al.*, Eds., vol. 36. Curran Associates, Inc., 2023, pp. 78126–78141.
- [43] R. Harb, T. Pock, and H. Müller, “Diffusion-based generation of histopathological whole slide images at a gigapixel scale,” 2023. [Online]. Available: <https://arxiv.org/abs/2311.08199>
- [44] C. Wang *et al.*, “Histology image artifact restoration with lightweight transformer based diffusion model,” in *Artificial Intelligence in Medicine*, J. Finkelstein, R. Moskovitch, and E. Parimbelli, Eds. Cham: Springer Nature Switzerland, 2024, pp. 81–89.
- [45] X. Xu, S. Kapse, and P. Prasanna, “Histo-diffusion: A diffusion super-resolution method for digital pathology with comprehensive quality assessment,” *CoRR*, vol. abs/2408.15218, 2024.
- [46] T. Kataria, B. Knudsen, and S. Y. Elhajian, “Staindiffuser: Multitask dual diffusion model for virtual staining,” 2024. [Online]. Available: <https://arxiv.org/abs/2403.11340>

- [47] X. Zheng *et al.*, “Diffusion-based virtual staining from polarimetric mueller matrix imaging,” 2025. [Online]. Available: <https://arxiv.org/abs/2503.01352>
- [48] R. Jewsbury *et al.*, “Stainfuser: Controlling diffusion for faster neural style transfer in multi-gigapixel histology images,” 2024. [Online]. Available: <https://arxiv.org/abs/2403.09302>
- [49] J. Jeong *et al.*, “Stain normalization using score-based diffusion model through stain separation and overlapped moving window patch strategies,” *Computers in Biology and Medicine*, vol. 152, p. 106335, 2023.
- [50] J. Ho and T. Salimans, “Classifier-free diffusion guidance,” *arXiv preprint arXiv:2207.12598*, 2022.
- [51] R. Rombach *et al.*, “High-resolution image synthesis with latent diffusion models,” in *Proceedings of the IEEE/CVF conference on computer vision and pattern recognition*, 2022, pp. 10 684–10 695.
- [52] L. Zhang, A. Rao, and M. Agrawala, “Adding conditional control to text-to-image diffusion models,” in *Proceedings of the IEEE/CVF international conference on computer vision*, 2023, pp. 3836–3847.
- [53] M. M. Ho *et al.*, “Disc: Latent diffusion models with self-distillation from separated conditions for prostate cancer grading,” in *2024 IEEE International Symposium on Biomedical Imaging (ISBI)*, 2024, pp. 1–5.
- [54] H. Zhang *et al.*, “Lefusion: Controllable pathology synthesis via lesion-focused diffusion models,” 2024. [Online]. Available: <https://arxiv.org/abs/2403.14066>
- [55] F. Carrillo-Perez *et al.*, “Generation of synthetic whole-slide image tiles of tumours from rna-sequencing data via cascaded diffusion models,” *Nature Biomedical Engineering*, vol. 9, no. 3, pp. 320–332, 03 2025.
- [56] Z. Liu *et al.*, “Generating progressive images from pathological transitions via diffusion model,” in *Medical Image Computing and Computer Assisted Intervention – MICCAI 2024*, M. G. Linguraru *et al.*, Eds. Cham: Springer Nature Switzerland, 2024, pp. 308–318.
- [57] L. Žigutytė *et al.*, “Counterfactual diffusion models for mechanistic explainability of artificial intelligence models in pathology,” *bioRxiv*, 2025, preprint. [Online]. Available: <https://doi.org/10.1101/2024.10.29.620913>
- [58] A. Radford *et al.*, “Learning transferable visual models from natural language supervision,” in *Proceedings of the 38th International Conference on Machine Learning*, ser. Proceedings of Machine Learning Research, M. Meila and T. Zhang, Eds., vol. 139. PMLR, 18–24 Jul 2021, pp. 8748–8763.
- [59] J. Devlin *et al.*, “BERT: Pre-training of deep bidirectional transformers for language understanding,” in *Proceedings of the 2019 Conference of the North American Chapter of the Association for Computational Linguistics: Human Language Technologies, Volume 1 (Long and Short Papers)*, J. Burstein, C. Doran, and T. Solorio, Eds. Minneapolis, Minnesota: Association for Computational Linguistics, jun 2019, pp. 4171–4186. [Online]. Available: <https://aclanthology.org/N19-1423/>
- [60] C. Jia *et al.*, “Scaling up visual and vision-language representation learning with noisy text supervision,” in *Proceedings of the 38th International Conference on Machine Learning*, ser. Proceedings of Machine Learning Research, M. Meila and T. Zhang, Eds., vol. 139. PMLR, 18–24 Jul 2021, pp. 4904–4916. [Online]. Available: <https://proceedings.mlr.press/v139/jia21b.html>
- [61] J.-B. Alayrac *et al.*, “Flamingo: a visual language model for few-shot learning,” in *Advances in Neural Information Processing Systems*, S. Koyejo *et al.*, Eds., vol. 35. Curran Associates, Inc., 2022, pp. 23 716–23 736.
- [62] J. Li *et al.*, “BLIP: Bootstrapping language-image pre-training for unified vision-language understanding and generation,” in *Proceedings of the 39th International Conference on Machine Learning*, ser. Proceedings of Machine Learning Research, K. Chaudhuri *et al.*, Eds., vol. 162. PMLR, 17–23 Jul 2022, pp. 12 888–12 900.
- [63] F. Ahmed *et al.*, “Pathalign: A vision–language model for whole slide images in histopathology,” in *MICCAI Workshop on Computational Pathology with Multimodal Data (COMPAYL)*, 2024. [Online]. Available: <https://openreview.net/forum?id=Q2nSLk9hKT>
- [64] S. Javed *et al.*, “Cclip: Zero-shot learning for histopathology with comprehensive vision-language alignment,” in *2024 IEEE/CVF Conference on Computer Vision and Pattern Recognition (CVPR)*, 2024, pp. 11 450–11 459.
- [65] H. Watawana *et al.*, “Hierarchical text-to-vision self supervised alignment for improved histopathology representation learning,” in *Medical Image Computing and Computer Assisted Intervention – MICCAI 2024*, M. G. Linguraru *et al.*, Eds. Cham: Springer Nature Switzerland, 2024, pp. 167–177.
- [66] S. Kim *et al.*, “Cosmos: Cross-modality self-distillation for vision language pre-training,” 2025. [Online]. Available: <https://arxiv.org/abs/2412.01814>
- [67] R. Lucassen *et al.*, “Preprocessing pathology reports for vision-language model development,” in *MICCAI Workshop on Computational Pathology with Multimodal Data (COMPAYL)*, 2024. [Online]. Available: <https://openreview.net/forum?id=SUgnMdiJ2q>
- [68] A.-T. Nguyen *et al.*, “Mgpath: Vision-language model with multi-granular prompt learning for few-shot wsi classification,” 2025. [Online]. Available: <https://arxiv.org/abs/2502.07409>
- [69] D. Nechaev, A. Pchel'nikov, and E. Ivanova, “Hibou: A family of foundational vision transformers for pathology,” *CoRR*, vol. abs/2406.05074, 2024. [Online]. Available: <https://doi.org/10.48550/arXiv.2406.05074>
- [70] D. Dai *et al.*, “Pa-llava: A large language-vision assistant for human pathology image understanding,” *CoRR*, vol. abs/2408.09530, 2024. [Online]. Available: <https://doi.org/10.48550/arXiv.2408.09530>
- [71] Y. Chen *et al.*, “Slidechat: A large vision-language assistant for whole-slide pathology image understanding,” 2024. [Online]. Available: <https://openreview.net/forum?id=Ng4HaH4L6P>
- [72] D. Dai *et al.*, “Pathologyvlm: a large vision-language model for pathology image understanding,” *Artificial Intelligence Review*, vol. 58, no. 6, p. 186, 03 2025, available at: <https://github.com/ddw2AIGROUP2CQUPT/PA-LLaVA>. [Online]. Available: <https://doi.org/10.1007/s10462-025-11190-1>
- [73] K. Chen *et al.*, “Cost-effective instruction learning for pathology vision and language analysis,” 2024. [Online]. Available: <https://arxiv.org/abs/2407.17734>
- [74] S. Sengupta and D. E. Brown, “Automatic report generation for histopathology images using pre-trained vision transformers and bert,” 2024. [Online]. Available: <https://arxiv.org/abs/2312.01435>
- [75] U. Naseem, M. Khushi, and J. Kim, “Vision-language transformer for interpretable pathology visual question answering,” *IEEE Journal of Biomedical and Health Informatics*, vol. 27, no. 4, pp. 1681–1690, 2023.
- [76] J. Xiang *et al.*, “A vision–language foundation model for precision oncology,” *Nature*, vol. 638, no. 8051, pp. 769–778, February 2025.
- [77] Y. Zhang *et al.*, “Dscenet: Dynamic screening and clinical-enhanced multimodal fusion for mpns subtype classification,” in *International Conference on Medical Image Computing and Computer-Assisted Intervention*. Springer, 2024, pp. 69–79.
- [78] R. Ding *et al.*, “Improving mitosis detection on histopathology images using large vision-language models,” in *2024 IEEE International Symposium on Biomedical Imaging (ISBI)*, 2024, pp. 1–5.
- [79] P. Thota *et al.*, “Demonstration of an adversarial attack against a multimodal vision language model for pathology imaging,” *21st IEEE International Symposium on Biomedical Imaging (ISBI 2024)*, 2024.
- [80] D. P. Kingma and M. Welling, “An introduction to variational autoencoders,” *Foundations and Trends® in Machine Learning*, vol. 12, no. 4, p. 307–392, 2019. [Online]. Available: <http://dx.doi.org/10.1561/22000000056>
- [81] D. J. Rezende and S. Mohamed, “Variational inference with normalizing flows,” 2016. [Online]. Available: <https://arxiv.org/abs/1505.05770>
- [82] J. Boyd *et al.*, “Self-supervised representation learning using visual field expansion on digital pathology,” in *2021 IEEE/CVF International Conference on Computer Vision Workshops (ICCVW)*, 2021, pp. 639–647.
- [83] K. Tang *et al.*, “Self-supervised representation distribution learning for reliable data augmentation in histopathology wsi classification,” *IEEE Transactions on Medical Imaging*, vol. 44, no. 1, pp. 462–474, 2025.
- [84] J. Zhou *et al.*, “Robust multimodal survival prediction with the latent differentiation conditional variational autoencoder,” 2025. [Online]. Available: <https://arxiv.org/abs/2503.09496>
- [85] A. van den Oord, N. Kalchbrenner, and K. Kavukcuoglu, “Pixel recurrent neural networks,” 2016. [Online]. Available: <https://arxiv.org/abs/1601.06759>
- [86] A. Radford *et al.*, “Improving language understanding by generative pre-training,” 2018.
- [87] A. Golfe *et al.*, “Enhancing image retrieval performance with generative models in siamese networks,” *IEEE Journal of Biomedical and Health Informatics*, vol. PP, 2025, advance online publication. [Online]. Available: <https://doi.org/10.1109/JBHI.2025.3543907>
- [88] P. Saremi *et al.*, “R14med-ddpo: Reinforcement learning for controlled guidance towards diverse medical image generation using vision-language foundation models,” 2025. [Online]. Available: <https://arxiv.org/abs/2503.15784>
- [89] Z. Xu *et al.*, “Hybrid reinforced medical report generation with m-linear attention and repetition penalty,” *IEEE Transactions on Neural Networks and Learning Systems*, vol. 36, no. 2, pp. 2206–2220, 2025.

- [90] W. Chen et al., "Star-rl: Spatial-temporal hierarchical reinforcement learning for interpretable pathology image super-resolution," *IEEE Transactions on Medical Imaging*, vol. 43, no. 12, pp. 4368–4379, 2024.
- [91] Y. Xue et al., "Selective synthetic augmentation with histogan for improved histopathology image classification," *Medical image analysis*, vol. 67, p. 101816, 2021.
- [92] A. Lahiani et al., "Seamless virtual whole slide image synthesis and validation using perceptual embedding consistency," *IEEE Journal of Biomedical and Health Informatics*, vol. 25, no. 2, pp. 403–411, 2021.
- [93] T. de Bel et al., "Residual cyclegan for robust domain transformation of histopathological tissue slides," *Medical Image Analysis*, vol. 70, p. 102004, 2021. [Online]. Available: <https://www.sciencedirect.com/science/article/pii/S1361841521000505>
- [94] A. C. Quiros, R. Murray-Smith, and K. Yuan, "Pathologygan: Learning deep representations of cancer tissue," 2021.
- [95] S. Butte et al., "Sharp-gan: Sharpness loss regularized gan for histopathology image synthesis," in *2022 IEEE 19th International symposium on biomedical imaging (ISBI)*. IEEE, 2022, pp. 1–5.
- [96] J. Ye et al., "A multi-attribute controllable generative model for histopathology image synthesis," in *Medical Image Computing and Computer Assisted Intervention – MICCAI 2021: 24th International Conference, Strasbourg, France, September 27–October 1, 2021, Proceedings, Part VIII 24*. Springer, 2021, pp. 613–623.
- [97] M. Tsuneki and F. Kanavati, "Inference of captions from histopathological patches," in *International Conference on Medical Imaging with Deep Learning*. PMLR, 2022, pp. 1235–1250.
- [98] A. B. Levine et al., "Synthesis of diagnostic quality cancer pathology images by generative adversarial networks," *The Journal of pathology*, vol. 252, no. 2, pp. 178–188, 2020.
- [99] V. Porter et al., "Optimising diffusion models for histopathology image synthesis," in *The British Machine Vision Conference*. BMVC, 2024.
- [100] P. A. Moghadam et al., "A morphology focused diffusion probabilistic model for synthesis of histopathology images," in *Proceedings of the IEEE/CVF Winter Conference on Applications of Computer Vision (WACV)*, January 2023, pp. 2000–2009.
- [101] X. Xu et al., "Vit-dae: Transformer-driven diffusion autoencoder for histopathology image analysis," in *International Conference on Medical Image Computing and Computer-Assisted Intervention*. Springer, 2023, pp. 66–76.
- [102] K. Ding et al., "A large-scale synthetic pathological dataset for deep learning-enabled segmentation of breast cancer," *Scientific Data*, vol. 10, no. 1, p. 231, 2023.
- [103] A. Golfe et al., "Progleason-gan: Conditional progressive growing gan for prostatic cancer gleason grade patch synthesis," *Computer Methods and Programs in Biomedicine*, vol. 240, p. 107695, 2023.
- [104] Z. He et al., "Artifact restoration in histology images with diffusion probabilistic models," in *Medical Image Computing and Computer Assisted Intervention – MICCAI 2023*, H. Greenspan et al., Eds. Cham: Springer Nature Switzerland, 2023, pp. 518–527.
- [105] S. Cechnicka et al., "Realistic data enrichment for robust image segmentation in histopathology," in *MICCAI Workshop on Domain Adaptation and Representation Transfer*. Springer, 2023, pp. 63–72.
- [106] S. Yellapragada et al., "Pathldm: Text conditioned latent diffusion model for histopathology," 2023. [Online]. Available: <https://arxiv.org/abs/2309.00748>
- [107] Y. Shen and J. Ke, "Staindiff: Transfer stain styles of histology images with denoising diffusion probabilistic models and self-ensemble," in *Medical Image Computing and Computer Assisted Intervention – MICCAI 2023*, H. Greenspan et al., Eds. Cham: Springer Nature Switzerland, 2023, pp. 549–559.
- [108] J. Linmans et al., "Diffusion models for out-of-distribution detection in digital pathology," *Medical Image Analysis*, vol. 93, p. 103088, 2024.
- [109] I. Ktena et al., "Generative models improve fairness of medical classifiers under distribution shifts," *Nature Medicine*, vol. 30, no. 4, pp. 1166–1173, 2024.
- [110] N. Sridhar et al., "Diffusion models for generative histopathology," in *Deep Generative Models*, A. Mukhopadhyay et al., Eds. Cham: Springer Nature Switzerland, 2024, pp. 154–163.
- [111] A. Graikos et al., "Learned representation-guided diffusion models for large-image generation," 2024. [Online]. Available: <https://arxiv.org/abs/2312.07330>
- [112] M. M. Ho et al., "F2fldm: Latent diffusion models with histopathology pre-trained embeddings for unpaired frozen section to fpe translation," 2024. [Online]. Available: <https://arxiv.org/abs/2404.12650>
- [113] Z. Li et al., "Av-gan: Attention-based varifocal generative adversarial network for uneven medical image translation," in *2024 International Joint Conference on Neural Networks (IJCNN)*, 2024, pp. 1–8.
- [114] S. Dubey et al., "Vims: virtual immunohistochemistry multiplex staining via text-to-stain diffusion trained on uniplex stains," in *International Workshop on Machine Learning in Medical Imaging*. Springer, 2024, pp. 143–155.
- [115] D. Reisenbüchler et al., "Unsupervised latent stain adaptation for computational pathology," in *International Conference on Medical Image Computing and Computer-Assisted Intervention*. Springer, 2024, pp. 755–765.
- [116] J. Li et al., "Pathup: Patch-wise timestep tracking for multi-class large pathology image synthesising diffusion model," in *Proceedings of the 32nd ACM International Conference on Multimedia*, 2024, pp. 3984–3993.
- [117] P. Pati et al., "Accelerating histopathology workflows with generative ai-based virtually multiplexed tumour profiling," *Nature Machine Intelligence*, vol. 6, pp. 1077–1093, 2024. [Online]. Available: <https://doi.org/10.1038/s42256-024-00889-5>
- [118] S. Cechnicka et al., "Urcdm: Ultra-resolution image synthesis in histopathology," in *International Conference on Medical Image Computing and Computer-Assisted Intervention*. Springer, 2024, pp. 535–545.
- [119] X. Xu, S. Kapse, and P. Prasanna, "Histo-diffusion: A diffusion super-resolution method for digital pathology with comprehensive quality assessment," *arXiv preprint arXiv:2408.15218*, 2024.
- [120] C.-C. Tsai, Y.-C. Chen, and C.-S. Lu, "Test-time stain adaptation with diffusion models for histopathology image classification," in *Computer Vision – ECCV 2024*, A. Leonardis et al., Eds. Cham: Springer Nature Switzerland, 2025, pp. 257–275.
- [121] J. Wang and J. Kwak, "Usegmix: Unsupervised segment mix for efficient data augmentation in pathology images," in *MICCAI Workshop on Data Engineering in Medical Imaging*. Springer, 2024, pp. 54–63.
- [122] Y. He et al., "Pst-diff: Achieving high-consistency stain transfer by diffusion models with pathological and structural constraints," *IEEE Trans. Medical Imaging*, vol. 43, no. 10, pp. 3634–3647, 2024. [Online]. Available: <https://doi.org/10.1109/TMI.2024.3430825>
- [123] W. Lou et al., "Multi-modal denoising diffusion pre-training for whole-slide image classification," in *Proceedings of the 32nd ACM International Conference on Multimedia*, ser. MM '24. New York, NY, USA: Association for Computing Machinery, 2024, p. 10804–10813. [Online]. Available: <https://doi.org/10.1145/3664647.3680882>
- [124] S. Liu et al., "Generating seamless virtual immunohistochemical whole slide images with content and color consistency," *arXiv preprint arXiv:2410.01072*, 2024.
- [125] Z. He et al., "Latentartifusion: An effective and efficient histological artifacts restoration framework," in *MICCAI Workshop on Deep Generative Models*. Springer, 2024, pp. 202–211.
- [126] M. Öttl et al., "Style-extracting diffusion models for semi-supervised histopathology segmentation," in *European Conference on Computer Vision*. Springer, 2024, pp. 236–252.
- [127] X. Zhang et al., "Hadiff: hierarchy aggregated diffusion model for pathology image segmentation," *The Visual Computer*, pp. 1–12, 2025.
- [128] M. Pozzi et al., "Generating and evaluating synthetic data in digital pathology through diffusion models," *Scientific Reports*, vol. 14, no. 1, p. 28435, 11 2024.
- [129] D. Thakkar et al., "Comparative analysis of diffusion generative models in computational pathology," *arXiv preprint arXiv:2411.15719*, 2024.
- [130] X. Yan et al., "Versatile stain transfer in histopathology using a unified diffusion framework," *bioRxiv*, 2024. [Online]. Available: <https://www.biorxiv.org/content/early/2024/11/23/2024.11.23.624680>
- [131] B. Xiong et al., "Unpaired multi-domain histopathology virtual staining using dual path prompted inversion," *Proceedings of the AAAI Conference on Artificial Intelligence*, vol. 39, no. 8, pp. 8780–8787, Apr. 2025. [Online]. Available: <https://ojs.aaai.org/index.php/AAAI/article/view/32949>
- [132] D. Winter et al., "Mask-guided cross-image attention for zero-shot in-silico histopathologic image generation with a diffusion model," 2025. [Online]. Available: <https://arxiv.org/abs/2407.11664>
- [133] J. Wang et al., "A value mapping virtual staining framework for large-scale histological imaging," *CoRR*, vol. abs/2501.03592, 2025. [Online]. Available: <https://doi.org/10.48550/arXiv.2501.03592>
- [134] M. Jehanzaib et al., "A robust image segmentation and synthesis pipeline for histopathology," *Medical Image Analysis*, vol. 99, p. 103344, 2025.
- [135] V. Purma et al., "Genselfdiff-his: Generative self-supervision using diffusion for histopathological image segmentation," *CoRR*, vol.

- abs/2309.01487, 2023. [Online]. Available: <https://doi.org/10.48550/arXiv.2309.01487>
- [136] J. Li *et al.*, “Topofm: Topology-guided pathology foundation model for high-resolution pathology image synthesis with cellular-level control,” *IEEE Transactions on Medical Imaging*, 2025.
- [137] H. Liu *et al.*, “Pathpainter: Augmenting histopathology segmentation via tumor-aware inpainting,” *arXiv preprint arXiv:2503.04634*, 2025.
- [138] W.-H. Li *et al.*, “Pdseg: Patch-wise distillation and controllable image generation for weakly-supervised histopathology tissue segmentation,” in *ICASSP 2025-2025 IEEE International Conference on Acoustics, Speech and Signal Processing (ICASSP)*. IEEE, 2025, pp. 1–5.
- [139] Z. Liu *et al.*, “Generating progressive images from pathological transitions via diffusion model,” in *International Conference on Medical Image Computing and Computer-Assisted Intervention*. Springer, 2024, pp. 308–318.
- [140] L. Žigutytė *et al.*, “Counterfactual diffusion models for mechanistic explainability of artificial intelligence models in pathology,” *bioRxiv*, pp. 2024–10, 2025.
- [141] A. C. Quiros, R. Murray-Smith, and K. Yuan, “Pathologygan: Learning deep representations of cancer tissue,” *arXiv preprint arXiv:1907.02644*, 2019.
- [142] J. Boyd *et al.*, “Self-supervised representation learning using visual field expansion on digital pathology,” in *Proceedings of the IEEE/CVF International Conference on Computer Vision*, 2021, pp. 639–647.
- [143] M. Liang *et al.*, “Multi-scale self-attention generative adversarial network for pathology image restoration,” *The Visual Computer*, vol. 39, no. 9, pp. 4305–4321, 2023.
- [144] S. S. Ghahfarokhi *et al.*, “Deep learning for automated detection of breast cancer in deep ultraviolet fluorescence images with diffusion probabilistic model,” in *2024 IEEE International Symposium on Biomedical Imaging (ISBI)*, 2024, pp. 1–5.
- [145] W. Chen *et al.*, “Star-rl: Spatial-temporal hierarchical reinforcement learning for interpretable pathology image super-resolution,” *IEEE Transactions on Medical Imaging*, 2024.
- [146] Z. Du *et al.*, “Deeply supervised two stage generative adversarial network for stain normalization,” *Scientific Reports*, vol. 15, no. 1, p. 7068, 02 2025. [Online]. Available: <https://doi.org/10.1038/s41598-025-91587-8>
- [147] J. Jeong *et al.*, “Stain normalization using score-based diffusion model through stain separation and overlapped moving window patch strategies,” *Computers in Biology and Medicine*, vol. 152, p. 106335, 2023. [Online]. Available: <https://www.sciencedirect.com/science/article/pii/S0010482522010435>
- [148] R. Rong *et al.*, “Enhanced pathology image quality with restore-generative adversarial network,” *The American Journal of Pathology*, vol. 193, no. 4, pp. 404–416, 2023. [Online]. Available: <https://www.sciencedirect.com/science/article/pii/S0002944023000275>
- [149] N. Sridhar *et al.*, “Diffusion models for generative histopathology,” in *Deep Generative Models*, A. Mukhopadhyay *et al.*, Eds. Cham: Springer Nature Switzerland, 2024, pp. 154–163.
- [150] X. Yan *et al.*, “Versatile stain transfer in histopathology using a unified diffusion framework,” *bioRxiv*, 2024. [Online]. Available: <https://www.biorxiv.org/content/early/2024/11/23/2024.11.23.624680>
- [151] J. Gamper and N. Rajpoot, “Multiple instance captioning: Learning representations from histopathology textbooks and articles,” in *2021 IEEE/CVF Conference on Computer Vision and Pattern Recognition (CVPR)*, 2021, pp. 16544–16554.
- [152] C. Li *et al.*, “LLaVA-med: Training a large language-and-vision assistant for biomedicine in one day,” in *Thirty-seventh Conference on Neural Information Processing Systems Datasets and Benchmarks Track*, 2023.
- [153] W. Qin *et al.*, “What a whole slide image can tell? subtype-guided masked transformer for pathological image captioning,” 2023. [Online]. Available: <https://arxiv.org/abs/2310.20607>
- [154] M. S. Seyfioglu *et al.*, “Quilt-llava: Visual instruction tuning by extracting localized narratives from open-source histopathology videos,” in *Proceedings of the IEEE/CVF Conference on Computer Vision and Pattern Recognition (CVPR)*, June 2024, pp. 13 183–13 192.
- [155] M. Tran *et al.*, “Generating clinical-grade pathology reports from gigapixel whole slide images with histogpt,” *medRxiv*, 2024. [Online]. Available: <https://www.medrxiv.org/content/early/2024/06/19/2024.03.15.24304211>
- [156] Z. Guo *et al.*, “Histgen: Histopathology report generation via local-global feature encoding and cross-modal context interaction,” in *International Conference on Medical Image Computing and Computer-Assisted Intervention*. Springer, 2024, pp. 189–199.
- [157] P. Chen *et al.*, “WsiCaption: Multiple Instance Generation of Pathology Reports for Gigapixel Whole-Slide Images,” in *Proceedings of Medical Image Computing and Computer Assisted Intervention – MICCAI 2024*, vol. LNCS 15004. Springer Nature Switzerland, October 2024.
- [158] Y. Sun *et al.*, “Pathgen-1.6m: 1.6 million pathology image-text pairs generation through multi-agent collaboration,” 2024. [Online]. Available: <https://arxiv.org/abs/2407.00203>
- [159] M. Y. Lu *et al.*, “A multimodal generative ai copilot for human pathology,” *Nature*, vol. 634, no. 8033, pp. 466–473, 10 2024. [Online]. Available: <https://doi.org/10.1038/s41586-024-07618-3>
- [160] Q. Zhou *et al.*, “Pathm3: A multimodal multi-task multiple instance learning framework for whole slide image classification and captioning,” in *Medical Image Computing and Computer Assisted Intervention – MICCAI 2024*, M. G. Linguraru *et al.*, Eds. Cham: Springer Nature Switzerland, 2024, pp. 373–383.
- [161] X. Wu *et al.*, “Pathinsight: Instruction tuning of multimodal datasets and models for intelligence assisted diagnosis in histopathology,” 2024. [Online]. Available: <https://arxiv.org/abs/2408.07037>
- [162] D. Ferber *et al.*, “In-context learning enables multimodal large language models to classify cancer pathology images,” *Nature Communications*, vol. 15, no. 1, p. 10104, 11 2024. [Online]. Available: <https://doi.org/10.1038/s41467-024-51465-9>
- [163] P. Chen *et al.*, “Wsi-vqa: Interpreting whole slide images by generative visual question answering,” in *Computer Vision – ECCV 2024*, A. Leonardis *et al.*, Eds. Cham: Springer Nature Switzerland, 2025, pp. 401–417.
- [164] F. Ahmed *et al.*, “Polypath: Adapting a large multimodal model for multi-slide pathology report generation,” 2025. [Online]. Available: <https://arxiv.org/abs/2502.10536>
- [165] R. T. Lucassen *et al.*, “Pathology report generation and multimodal representation learning for cutaneous melanocytic lesions,” 2025. [Online]. Available: <https://arxiv.org/abs/2502.19293>
- [166] D. Hu *et al.*, “Pathology report generation from whole slide images with knowledge retrieval and multi-level regional feature selection,” *Computer Methods and Programs in Biomedicine*, vol. 263, p. 108677, 2025. [Online]. Available: <https://www.sciencedirect.com/science/article/pii/S016926072500094X>
- [167] F. Ghezloo *et al.*, “Pathfinder: A multi-modal multi-agent system for medical diagnostic decision-making applied to histopathology,” 2025. [Online]. Available: <https://arxiv.org/abs/2502.08916>
- [168] R. Saluja *et al.*, “Cancer type, stage and prognosis assessment from pathology reports using llms,” 2025. [Online]. Available: <https://arxiv.org/abs/2503.01194>
- [169] S. Elbedwehy *et al.*, “Enhanced descriptive captioning model for histopathological patches,” *Multimedia Tools and Applications*, vol. 83, no. 12, pp. 36 645–36 664, 04 2024. [Online]. Available: <https://doi.org/10.1007/s11042-023-15884-y>
- [170] X. He *et al.*, “Pathvqa: 30000+ questions for medical visual question answering,” 2020. [Online]. Available: <https://arxiv.org/abs/2003.10286>
- [171] M. Tran *et al.*, “Generating highly accurate pathology reports from gigapixel whole slide images with histogpt,” *medRxiv*, pp. 2024–03, 2024.
- [172] T. Tu *et al.*, “Towards generalist biomedical ai,” *NEJM AI*, vol. 1, no. 3, p. A10a2300138, 2024. [Online]. Available: <https://ai.nejm.org/doi/full/10.1056/A10a2300138>
- [173] M. Y. Lu *et al.*, “A visual-language foundation model for computational pathology,” *Nature Medicine*, vol. 30, no. 3, pp. 863–874, 2024. [Online]. Available: <https://doi.org/10.1038/s41591-024-02856-4>
- [174] Y. Sun *et al.*, “Pathasst: A generative foundation ai assistant towards artificial general intelligence of pathology,” *Proceedings of the AAAI Conference on Artificial Intelligence*, vol. 38, no. 5, pp. 5034–5042, Mar. 2024. [Online]. Available: <https://ojs.aaai.org/index.php/AAAI/article/view/28308>
- [175] G. Shaikovski *et al.*, “Prism: A multi-modal generative foundation model for slide-level histopathology,” 2024. [Online]. Available: <https://arxiv.org/abs/2405.10254>
- [176] C. Shen *et al.*, “Large-vocabulary forensic pathological analyses via prototypical cross-modal contrastive learning,” *arXiv preprint arXiv:2407.14904*, 2024.
- [177] J. Ma *et al.*, “Towards a generalizable pathology foundation model via unified knowledge distillation,” 2025. [Online]. Available: <https://arxiv.org/abs/2407.18449>
- [178] Y. Xu *et al.*, “A multimodal knowledge-enhanced whole-slide pathology foundation model,” 2025. [Online]. Available: <https://arxiv.org/abs/2407.15362>
- [179] S. Hua *et al.*, “Pathoduet: Foundation models for pathological slide analysis of h&e and ihc stains,” *Medical Image Analysis*, vol. 97,

- p. 103289, 2024. [Online]. Available: <https://www.sciencedirect.com/science/article/pii/S1361841524002147>
- [180] F. Yan *et al.*, “Pathorchestra: A comprehensive foundation model for computational pathology with over 100 diverse clinical-grade tasks,” 2025. [Online]. Available: <https://arxiv.org/abs/2503.24345>
- [181] F. Shahid *et al.*, “Using generative ai to extract structured information from free text pathology reports,” *Journal of Medical Systems*, vol. 49, no. 1, p. 36, 03 2025. [Online]. Available: <https://doi.org/10.1007/s10916-025-02167-2>
- [182] J. B. Balasubramanian *et al.*, “Leveraging large language models for structured information extraction from pathology reports,” 2025. [Online]. Available: <https://arxiv.org/abs/2502.12183>
- [183] X. Yang *et al.*, “Enhancing doctor-patient communication using large language models for pathology report interpretation,” *BMC Medical Informatics and Decision Making*, vol. 25, no. 1, p. 36, 01 2025. [Online]. Available: <https://doi.org/10.1186/s12911-024-02838-z>
- [184] Z. Huang *et al.*, “A visual-language foundation model for pathology image analysis using medical twitter,” *Nature Medicine*, vol. 29, no. 9, pp. 2307–2316, sep 2023. [Online]. Available: <https://doi.org/10.1038/s41591-023-02504-3>
- [185] M. Madeira, D. Thanou, and P. Frossard, “Tertiary lymphoid structures generation through graph-based diffusion,” in *Graphs in Biomedical Image Analysis, and Overlapped Cell on Tissue Dataset for Histopathology*, S.-A. Ahmadi and S. Pereira, Eds. Cham: Springer Nature Switzerland, 2024, pp. 37–53.
- [186] M. Sturm, L. Cerrone, and F. A. Hamprecht, “Syncellfactory: Generative data augmentation for cell tracking,” in *Medical Image Computing and Computer Assisted Intervention – MICCAI 2024*, M. G. Linguraru *et al.*, Eds. Cham: Springer Nature Switzerland, 2024, pp. 304–313.
- [187] X. Zhou *et al.*, “Knowledge-enhanced visual-language pretraining for computational pathology,” 2024. [Online]. Available: <https://arxiv.org/abs/2404.09942>
- [188] G. Jaume *et al.*, “Transcriptomics-guided slide representation learning in computational pathology,” in *Proceedings of the IEEE/CVF Conference on Computer Vision and Pattern Recognition*, 2024, pp. 9632–9644.
- [189] D. Juyal *et al.*, “Pluto: Pathology-universal transformer,” *arXiv preprint arXiv:2405.07905*, 2024.
- [190] C. Yin *et al.*, “Prompting vision foundation models for pathology image analysis,” in *Proceedings of the IEEE/CVF Conference on Computer Vision and Pattern Recognition*, 2024, pp. 11 292–11 301.
- [191] A. T. Nguyen, T. T. L. Vuong, and J. T. Kwak, “Towards a text-based quantitative and explainable histopathology image analysis,” in *Medical Image Computing and Computer Assisted Intervention – MICCAI 2024*, M. G. Linguraru *et al.*, Eds. Cham: Springer Nature Switzerland, 2024, pp. 514–524.
- [192] R. Bruch *et al.*, “Improving 3d deep learning segmentation with biophysically motivated cell synthesis,” 2024. [Online]. Available: <https://arxiv.org/abs/2408.16471>
- [193] C. Li *et al.*, “Spatial diffusion for cell layout generation,” in *Medical Image Computing and Computer Assisted Intervention – MICCAI 2024*, M. G. Linguraru *et al.*, Eds. Cham: Springer Nature Switzerland, 2024, pp. 481–491.
- [194] M. Xu *et al.*, “Topocellgen: Generating histopathology cell topology with a diffusion model,” 2025. [Online]. Available: <https://arxiv.org/abs/2412.06011>
- [195] K. Tang *et al.*, “Promptable representation distribution learning and data augmentation for gigapixel histopathology wsi analysis,” *Proceedings of the AAAI Conference on Artificial Intelligence*, vol. 39, no. 7, pp. 7247–7256, Apr. 2025. [Online]. Available: <https://ojs.aaai.org/index.php/AAAI/article/view/32779>
- [196] Z. Shao *et al.*, “Augdiff: Diffusion-based feature augmentation for multiple instance learning in whole slide image,” *IEEE Transactions on Artificial Intelligence*, vol. 5, no. 12, pp. 6617–6628, 2024.
- [197] J. Fan *et al.*, “Dcdiff: Dual-granularity cooperative diffusion models for pathology image analysis,” *IEEE Transactions on Medical Imaging*, vol. 43, no. 12, pp. 4393–4403, 2024.
- [198] J. Zhou *et al.*, “Damm-diffusion: Learning divergence-aware multimodal diffusion model for nanoparticles distribution prediction,” 2025. [Online]. Available: <https://arxiv.org/abs/2503.09491>
- [199] A. Vaidya *et al.*, “Molecular-driven foundation model for oncologic pathology,” 2025. [Online]. Available: <https://arxiv.org/abs/2501.16652>
- [200] S. Zhu *et al.*, “Diffusion generative modeling for spatially resolved gene expression inference from histology images,” 2025. [Online]. Available: <https://arxiv.org/abs/2501.15598>
- [201] Q. Zhou *et al.*, “Mllm4pue: Toward universal embeddings in digital pathology through multimodal llms,” 2025. [Online]. Available: <https://arxiv.org/abs/2502.07221>
- [202] Y. Sun *et al.*, “Pathmmu: A massive multimodal expert-level benchmark for understanding and reasoning in pathology,” 2024. [Online]. Available: <https://arxiv.org/abs/2401.16355>
- [203] P. Weitz *et al.*, “Acrobat – a multi-stain breast cancer histological whole-slide-image data set from routine diagnostics for computational pathology,” 2022. [Online]. Available: <https://arxiv.org/abs/2211.13621>
- [204] S. Liu *et al.*, “Bci: Breast cancer immunohistochemical image generation through pyramid pix2pix,” in *Proceedings of the IEEE/CVF Conference on Computer Vision and Pattern Recognition (CVPR) Workshops*, June 2022, pp. 1815–1824.
- [205] S. Karkampouna and M. Kruihof-de Julio, “Dataset empact tma,” Nov. 2023. [Online]. Available: <https://doi.org/10.5281/zenodo.10066853>
- [206] J. Gamper and N. Rajpoot, “Multiple instance captioning: Learning representations from histopathology textbooks and articles,” in *Proceedings of the IEEE conference on computer vision and pattern recognition*, 2021.
- [207] B. Ehteshami Bejnordi *et al.*, “Diagnostic assessment of deep learning algorithms for detection of lymph node metastases in women with breast cancer,” *JAMA*, vol. 318, no. 22, pp. 2199–2210, 12 2017. [Online]. Available: <https://doi.org/10.1001/jama.2017.14585>
- [208] Q. Da *et al.*, “Digestpath: A benchmark dataset with challenge review for the pathological detection and segmentation of digestive-system,” *Medical Image Analysis*, vol. 80, p. 102485, 2022. [Online]. Available: <https://www.sciencedirect.com/science/article/pii/S1361841522001323>
- [209] S. Graham *et al.*, “Conic challenge: Pushing the frontiers of nuclear detection, segmentation, classification and counting,” 2023. [Online]. Available: <https://arxiv.org/abs/2303.06274>
- [210] —, “Hover-net: Simultaneous segmentation and classification of nuclei in multi-tissue histology images,” *Medical Image Analysis*, vol. 58, p. 101563, 2019.
- [211] J. Gamper *et al.*, “Pannuke: an open pan-cancer histology dataset for nuclei instance segmentation and classification,” in *European Congress on Digital Pathology*. Springer, 2019, pp. 11–19.
- [212] M. Amgad *et al.*, “Structured crowdsourcing enables convolutional segmentation of histology images,” *Bioinformatics*, vol. 35, no. 18, pp. 3461–3467, 02 2019. [Online]. Available: <https://doi.org/10.1093/bioinformatics/btz083>
- [213] K. Sirinukunwattana *et al.*, “Gland segmentation in colon histology images: The glas challenge contest,” 2016. [Online]. Available: <https://arxiv.org/abs/1603.00275>
- [214] S. Graham *et al.*, “Lizard: A large-scale dataset for colonic nuclear instance segmentation and classification,” in *Proceedings of the IEEE/CVF International Conference on Computer Vision*, 2021, pp. 684–693.
- [215] N. Kumar *et al.*, “A multi-organ nucleus segmentation challenge,” *IEEE Transactions on Medical Imaging*, vol. 39, no. 5, pp. 1380–1391, 2020.
- [216] D. Komura *et al.*, “Restaining-based annotation for cancer histology segmentation to overcome annotation-related limitations among pathologists,” *Patterns*, vol. 4, Feb. 2023. [Online]. Available: <https://doi.org/10.1016/j.patter.2023.100688>
- [217] C. Han *et al.*, “Wsss4luad: Grand challenge on weakly-supervised tissue semantic segmentation for lung adenocarcinoma,” arXiv, 2022.
- [218] K. Ding *et al.*, “A large-scale synthetic pathological dataset for deep learning-enabled segmentation of breast cancer,” Jun. 2022. [Online]. Available: <https://doi.org/10.5281/zenodo.6633721>
- [219] W. O. Ikezogwo *et al.*, “Quilt-1m: One million image-text pairs for histopathology,” Aug. 2023. [Online]. Available: <https://doi.org/10.5281/zenodo.8239942>
- [220] X. Zhang *et al.*, “Pmc-vqa: Visual instruction tuning for medical visual question answering,” 2024. [Online]. Available: <https://arxiv.org/abs/2305.10415>
- [221] M. Veta *et al.*, “Predicting breast tumor proliferation from whole-slide images: The tupac16 challenge,” *Medical Image Analysis*, vol. 54, pp. 111–121, 2019. [Online]. Available: <https://www.sciencedirect.com/science/article/pii/S1361841518305231>
- [222] G. Jaume *et al.*, “HEST-1k: A Dataset for Spatial Transcriptomics and Histology Image Analysis,” *arXiv*, Jun. 2024. [Online]. Available: <https://arxiv.org/abs/2406.16192v1>
- [223] N. Brancati *et al.*, “Bracs: A dataset for breast carcinoma subtyping in h&e histology images,” *Database*, vol. 2022, p. baac093, 10 2022. [Online]. Available: <https://doi.org/10.1093/database/baac093>
- [224] A. Naumov *et al.*, “Endonuke: Nuclei detection dataset for estrogen and progesterone stained ihc endometrium scans,” *Data*, vol. 7, no. 6, 2022. [Online]. Available: <https://www.mdpi.com/2306-5729/7/6/75>

- [225] A. Polónia, C. Eloy, and P. Aguiar, "Bach dataset : Grand challenge on breast cancer histology images," May 2019. [Online]. Available: <https://doi.org/10.5281/zenodo.3632035>
- [226] F. Xu *et al.*, "Predicting axillary lymph node metastasis in early breast cancer using deep learning on primary tumor biopsy slides," *Frontiers in Oncology*, p. 4133, 2021.
- [227] F. A. Spanhol *et al.*, "A dataset for breast cancer histopathological image classification," *IEEE Transactions on Biomedical Engineering*, vol. 63, no. 7, pp. 1455–1462, 2016.
- [228] P. Bándi *et al.*, "From detection of individual metastases to classification of lymph node status at the patient level: The camelyon17 challenge," *IEEE Transactions on Medical Imaging*, vol. 38, no. 2, pp. 550–560, 2019.
- [229] J. N. Kather, N. Halama, and A. Marx, "100,000 histological images of human colorectal cancer and healthy tissue," Apr. 2018. [Online]. Available: <https://doi.org/10.5281/zenodo.1214456>
- [230] S. Farahmand *et al.*, "HER2 and trastuzumab treatment response H&E slides with tumor ROI annotations (Version 3)," 2022. [Online]. Available: <https://doi.org/10.7937/E65C-AM96>
- [231] T. Araújo *et al.*, "Classification of breast cancer histology images using convolutional neural networks," *PLOS ONE*, vol. 12, no. 6, pp. 1–14, 06 2017. [Online]. Available: <https://doi.org/10.1371/journal.pone.0177544>
- [232] A. A. Borkowski *et al.*, "Lc25000 lung and colon histopathological image dataset." [Online]. Available: [https://github.com/tampapath/lung\\_colon\\_image\\_set](https://github.com/tampapath/lung_colon_image_set)
- [233] J. Wei *et al.*, "A petri dish for histopathology image analysis," in *International Conference on Artificial Intelligence in Medicine*. Springer, 2021, pp. 11–24.
- [234] W. Bulten *et al.*, "Artificial intelligence for diagnosis and gleason grading of prostate cancer: the panda challenge," *Nature Medicine*, 2022. [Online]. Available: <https://doi.org/10.1038/s41591-021-01620-2>
- [235] B. S. Veeling *et al.*, "Rotation equivariant cnns for digital pathology," Sep. 2018. [Online]. Available: [https://doi.org/10.1007/978-3-030-00934-2\\_24](https://doi.org/10.1007/978-3-030-00934-2_24)
- [236] J. Silva-Rodríguez, "SICAPv2 - Prostate Whole Slide Images with Gleason Grades Annotations," 2020.
- [237] M. Tsuneki and F. Kanavati, "Patchgastricadc22," Dec. 2021. [Online]. Available: <https://doi.org/10.5281/zenodo.6021442>
- [238] M. Heusel *et al.*, "Gans trained by a two time-scale update rule converge to a local nash equilibrium," *Advances in neural information processing systems*, vol. 30, 2017.
- [239] Z. Wang *et al.*, "Patch diffusion: Faster and more data-efficient training of diffusion models," *Advances in neural information processing systems*, vol. 36, pp. 72 137–72 154, 2023.
- [240] S. Barratt and R. Sharma, "A note on the inception score," *arXiv preprint arXiv:1801.01973*, 2018.
- [241] R. Zhang *et al.*, "The unreasonable effectiveness of deep features as a perceptual metric," in *Proceedings of the IEEE conference on computer vision and pattern recognition*, 2018, pp. 586–595.
- [242] Z. Wang *et al.*, "Image quality assessment: from error visibility to structural similarity," *IEEE transactions on image processing*, vol. 13, no. 4, pp. 600–612, 2004.
- [243] L. Zhang *et al.*, "Fsim: A feature similarity index for image quality assessment," *IEEE transactions on Image Processing*, vol. 20, no. 8, pp. 2378–2386, 2011.
- [244] W. Xue *et al.*, "Gradient magnitude similarity deviation: A highly efficient perceptual image quality index," *IEEE transactions on image processing*, vol. 23, no. 2, pp. 684–695, 2013.
- [245] R. Vedantam, C. Lawrence Zitnick, and D. Parikh, "Cider: Consensus-based image description evaluation," in *Proceedings of the IEEE conference on computer vision and pattern recognition*, 2015, pp. 4566–4575.
- [246] J. Piper, "Luminance contrast, a new illumination technique in light microscopy: optical basics, practical evaluations, further developments," *Optik*, vol. 120, no. 18, pp. 963–975, 2009.
- [247] Z. Wang and A. C. Bovik, "Mean squared error: Love it or leave it? a new look at signal fidelity measures," *IEEE signal processing magazine*, vol. 26, no. 1, pp. 98–117, 2009.
- [248] A. De Myttenaere *et al.*, "Mean absolute percentage error for regression models," *Neurocomputing*, vol. 192, pp. 38–48, 2016.
- [249] B. Zhang and R. Sennrich, "Root mean square layer normalization," *Advances in Neural Information Processing Systems*, vol. 32, 2019.
- [250] J. Korhonen and J. You, "Peak signal-to-noise ratio revisited: Is simple beautiful?" in *2012 Fourth international workshop on quality of multimedia experience*. IEEE, 2012, pp. 37–38.
- [251] G. Fasano and A. Franceschini, "A multidimensional version of the kolmogorov–smirnov test," *Monthly Notices of the Royal Astronomical Society*, vol. 225, no. 1, pp. 155–170, 1987.
- [252] S. Vallender, "Calculation of the wasserstein distance between probability distributions on the line," *Theory of Probability & Its Applications*, vol. 18, no. 4, pp. 784–786, 1974.
- [253] P. W. Lambert *et al.*, "Jensen-shannon divergence: A multipurpose distance for statistical and quantum mechanics," in *AIP Conference Proceedings*, vol. 913, no. 1. American Institute of Physics, 2007, pp. 32–37.
- [254] J. R. Hershey and P. A. Olsen, "Approximating the kullback leibler divergence between gaussian mixture models," in *2007 IEEE International Conference on Acoustics, Speech and Signal Processing-ICASSP'07*, vol. 4. IEEE, 2007, pp. IV–317.
- [255] K. M. Borgwardt *et al.*, "Integrating structured biological data by kernel maximum mean discrepancy," *Bioinformatics*, vol. 22, no. 14, pp. e49–e57, 2006.
- [256] M. Bińkowski *et al.*, "Demystifying mmd gans," in *International Conference on Learning Representations*, 2018.
- [257] H. Rezatofighi *et al.*, "Generalized intersection over union: A metric and a loss for bounding box regression," in *Proceedings of the IEEE/CVF conference on computer vision and pattern recognition*, 2019, pp. 658–666.
- [258] I. Cohen *et al.*, "Pearson correlation coefficient," *Noise reduction in speech processing*, pp. 1–4, 2009.
- [259] R. Raskar and M. Cohen, "Image precision silhouette edges," in *Proceedings of the 1999 symposium on Interactive 3D graphics*, 1999, pp. 135–140.
- [260] D. F. Marks, "Visual imagery differences in the recall of pictures," *British journal of Psychology*, vol. 64, no. 1, pp. 17–24, 1973.
- [261] K. Papineni *et al.*, "Bleu: a method for automatic evaluation of machine translation," in *Proceedings of the 40th annual meeting of the Association for Computational Linguistics*, 2002, pp. 311–318.
- [262] C. Lin, "Recall-oriented understudy for gisting evaluation (rouge)," *Retrieved August*, vol. 20, p. 2005, 2005.
- [263] S. Banerjee and A. Lavie, "Meteor: An automatic metric for mt evaluation with improved correlation with human judgments," in *Proceedings of the acl workshop on intrinsic and extrinsic evaluation measures for machine translation and/or summarization*, 2005, pp. 65–72.
- [264] M. L. Bellon-Harn *et al.*, "Speech-language pathologists' preferences for patient-centeredness," *Journal of Communication Disorders*, vol. 68, pp. 81–88, 2017.
- [265] S. Hao *et al.*, "Synthetic data in ai: Challenges, applications, and ethical implications," *arXiv preprint arXiv:2401.01629*, 2024.
- [266] E. Zimmermann *et al.*, "Virchow2: Scaling self-supervised mixed magnification models in pathology," 2024. [Online]. Available: <https://arxiv.org/abs/2408.00738>